MASTER THESIS

THE EFFECT OF PARTNER PERFORMANCE ON ARM IMPEDANCE MODULATION DURING HAPTIC HUMAN-HUMAN INTERACTION

Eline Zwijgers

FACULTY OF ENGINEERING TECHNOLOGY
DEPARTMENT OF BIOMECHANICAL ENGINEERING

EXAMINATION COMMITTEE
dr. E.H.F. van Asseldonk
dr. ir. N.W.M. Beckers
prof. dr. ir. J.H. Buurke

DOCUMENT NUMBER
BW - 706

UNIVERSITY OF TWENTE.

29-10-2019

Contents

Chapter 1

General introduction

Intelligent systems are rapidly becoming ubiquitous in the modern healthcare system. Robotic devices assist surgeons in minimally invasive surgeries [1] and help therapists during neurorehabilitation and physical therapy [2, 3]. Besides, exoskeletons are used to support gait to retain lost motor functions [4]. The control of such robots is however a complex challenge [5]. Robotic devices are currently controlled in an ad-hoc manner based on classical control methodologies [2, 5] but in order to enhance the design of effective, versatile and intuitive interaction robots, researchers have expressed the desire to design robots that resemble interactions between two humans [2, 5, 6]. Interacting robots that resemble the interaction between humans could help us to better understand the intentions of the robot and vice-versa. Rehabilitation robots could interact with a patient just like a therapist would do in order to facilitate recovery and alleviate the demands of the therapist [5].

1.1 Human-human interaction

Human-human interaction happens through various physiological processes by exchanging signals with one another [7]. Speech is the most obvious means to establish interaction, but there are many others. Besides speech, humans are able to coordinate actions between each other through for instance facial expressions, body posture or gestures [8]. Facial expressions and body posture tell us something about someone's feelings [9] while monitoring body movements can be used to infer someone's intentions [10]. Humans can also coordinate actions by exerting forces onto each other. This type of interaction is referred to as physical human-human interaction or haptic human-human interaction (as haptic concerns touch and force) [11].

1.1.1 Haptic human-human interaction

Physical or haptic interaction occurs when two humans pass an object, move furniture, teach manual skills, or dance. Forces and motions are coupled either directly from limb to limb or via a mutually grasped object which can either be rigid or compliant. Physical interaction requires partners to adapt, anticipate, and react to each other's forces and motions [12]. The physical interaction between humans depends mainly on the task and roles of each partner [11, 5]. Jarrassé et al. [11] described a framework for the description of different types of haptic human-human interaction. The interactions are classified into three main categories: competition, collaboration and cooperation (see Fig. 1.1).

Competition

During a competition, both partners only concentrate on minimising their own cost (sum of effort and error) and, if necessary impede other's performance. While in competition, two humans may have different goals, such as reaching different targets at the same time with the same object, e.g. playing tug-of-war. Besides, humans may have the same goal, such as when two basketball players try to grasp for the ball.

Cooperation

Cooperation is a form of haptic human-human interaction in which each partner considers his/her own cost and that of their partner in order to work together towards a consensual solution to a problem. The roles in a cooperation are determined a priori and are fixed, such as a student-teacher relation.

Cooperative haptic interaction can be further subdivided into two groups: assistance and education. Assistance is a form of interaction in in which one partner is providing assistive forces to the other partner in order to achieve a motor goal that the second partner may not be able to accomplish on his or her own [5]. The assisting partner in this case only considers the cost of the partner who is receiving assistance. During education one partner (teacher) considers his/her own effort and the error of the other partner (student) while the student only considers his/her own cost. The goal of education is for the teacher to eventually become obsolete, allowing the student to perform the task independently.

Collaboration

Collaboration is, like cooperation, a form of haptic human-human interaction in which each partner considers his/her own cost and that of their partner in order to work together towards a consensual solution to a problem. However, during a collaboration, roles are not assigned a priori and can emerge and change spontaneously. Both partners attempt to achieve the task by themselves but could also take the performance of the other partner into account. Partners are equally responsible for reaching the goal, e.g. moving furniture or cycling a tandem together.

A form of collaboration is known as co-activity. During co-activity, partners can interact with one another to succeed in the common task without needing to know what the other partner is doing [11]. An example of co-activity is when two interacting partners are connected through a haptic connection while executing a motor task independently. Although they are ignoring their partner, they are influenced through the interaction force exchanged by the haptic connection [13]. Co-activity is the simplest form of haptic human-human interaction since exchange of haptic information through the interaction force is possible but yet not required.

1.1.2 Previous work on haptic human-human interaction

Research on haptic interaction between humans has mostly focused on collaboration. While collaboration tasks in daily life often involve whole-body movement such as folding a tablecloth, studies have focused primarily on visuomotor tasks that require limited degrees-of-freedom [5]. During most studies, participants sit across each other and face a computer screen while holding a manipulandum. This manipulandum provides either a direct physical haptic link [14] or virtual coupling [15]. The participants perform a joint motor task which could include real [14] or virtual [16] object manipulation or trajectory tracking [15]. During these tasks, participants obtain visual feedback in order to complete the task as quickly or as accurately as possible.

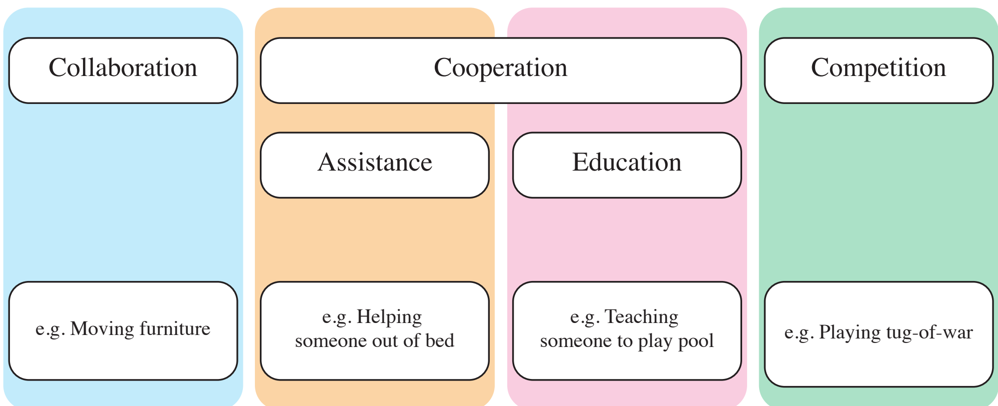

Figure 1.1: Taxonomy of haptic human-human interaction based upon the classification proposed by Jarrassé [11].

Improvement of performance due to haptic interaction

Two haptically coupled partners can perform a collaboration task as well as [17] or better than [14, 15] either of the partners alone. Ganesh et al. [15] performed a co-activity task in which two participants were compliantly coupled by a virtual spring during a tracking task. The target trajectory was the same for both participants. They showed that physically interacting participants improved, regardless of whether the partner performance was better or worse than the individual's performance. It is surprising that a better partner improves while being connected to a worse partner since you might expect that this connection would impede performance.

Haptic interaction strategies

Takagi et al. [18] explained the results of Ganesh et al. [15] by proposing that physically interacting partners continuously estimate each other's movement goal. They introduced the 'interpersonal goal integration' model in which partners use the interaction force to estimate the partner's movement goal by first estimating the partner's position and thereafter the control actions in order to improve motor performance. They compared the prediction of the interpersonal goal integration model and three other models, proposed in the literature, against data from an empirical physical interaction task. The other interaction models were the 'no computation model', the 'follow the better' model and the 'multi-sensory integration' model. The no computational model assumes that no haptic information is exchanged between partners. The follow the better model assumes that partners estimate each others performance through the haptic connection and switch to following the partner when he/she is better [19]. Finally, the multi-sensory integration model presumes that partners estimate each other's position through the haptic interaction force and optimally combine this information with their own information about the target position [20]. Takagi et al. found that the interpersonal goal integration model fitted the empirical data best. However, other haptic interaction strategies might be adopted and responsible for improvement during interaction.

Mojtahedi et al. [21] for instance showed that a partner ('follower') was able to infer the intended or imagined (but not executed) movement direction from the upper limb impedance of the other partner ('leader') while being rigidly coupled to each other. The follower was instructed to scan the workspace while the leader was instructed to stay within the centre of the workspace while preserving the intention to move in a given intended direction. This study suggests that the modulation of joint impedance might be a contributor of haptic communication in haptic human-human interaction.

1.2 Joint impedance

Joint impedance relates the position of the joint and the torque acting on it. The control of joint impedance allows the central nervous system to vary the resistance to forces applied to the body and to provide stability [22, 23]. In everyday life, we often need to reject external disturbances or perform manipulative tasks that involve unstable interactions between the body and the environment, e.g. when handling tools [24]. To successfully perform these actions, the joint impedance must be controlled because it stabilises the limb to external force fields [25, 26]. A higher joint impedance suppresses the effects of internal noise on movement kinematics and is therefore one of the strategies used by the neuromuscular system to generate accurate movements [27, 28, 29, 30, 31]. Besides, joint impedance is a mechanism used in the early phase of learning to accelerate the rate of dynamic motor learning [26, 32] and decreases as an internal model is formed [33].

1.2.1 Modulation of joint impedance

Joint impedance consists of three contributions [34, 35, 36]:

1. an intrinsic contribution due to limb inertia and the viscoelastic properties of muscle fibres and tissues in rest;
2. an intrinsic contribution due to active muscle fibres;
3. a reflexive contribution were muscles respond to stretches by producing counteracting torques.

Because of the large range over which it can be modulated, muscle activation is used to profoundly alter joint impedance.

Muscles are arranged in antagonistic groups of muscles which control the motion of a body segment about a joint. The body segment is accelerated by one group of muscles in one direction while the other group of muscles accelerates the body segment in the opposite direction. The muscles that accelerate the body segment in the direction of motion are referred to as agonists of the movement whereas the decelerating muscles are referred to as antagonists of the movement [37]. For instance, the biceps brachii and the triceps brachii form an agonist/antagonist muscle pair in which the biceps brachii causes flexion of the elbow joint whereas the triceps brachii causes extension of the elbow joint.

The net torque about a joint is determined by the difference between the activities of the agonist and antagonist muscles and are thus subtracted from one another. As muscles are activated to generate a torque, joint impedance changes. This is because muscle activation increases the stiffness [38, 39, 40] and to a lesser degree the viscosity [38, 39, 41] of a joint. Both stiffness and viscosity increase linearly as muscle activation increases [37]. In contrast to joint torque, joint impedance is predominantly determined by the sum of the activities of the agonist and antagonist muscles [39]. Equal activation of agonist and antagonist muscles, referred to as co-contraction, are thus responsible for increasing joint impedance without changing the net torque [24]. Hence, humans are capable of modulating joint impedance independent of torque through a change in muscle co-contraction.

Bibliography

[1] F. Guo, D. Ma, and S. Li, "Compare the prognosis of da vinci robot-assisted thoracic surgery (rats) with video-assisted thoracic surgery (vats) for non-small cell lung cancer: A meta-analysis," *Medicine*, vol. 98, no. 39, 2019.

[2] L. Marchal-Crespo and D. J. Reinkensmeyer, "Review of control strategies for robotic movement training after neurologic injury," *Journal of NeuroEngineering and Rehabilitation*, vol. 6, no. 1, 2009.

[3] P. T. K. J. Mehrholz, J and M. Pohl, "Electromechanical and robot-assisted arm training for improving arm function and activities of daily living after stroke," *Cochrane Database of Systematic Reviews*, no. 4, 2008.

[4] A. Esquenazi, M. Talaty, A. Packel, and M. Saulino, "The rewalk powered exoskeleton to restore ambulatory function to individuals with thoracic-level motor-complete spinal cord injury," *American Journal of Physical Medicine & Rehabilitation*, vol. 91, no. 11, pp. 911–921, 2012.

[5] A. Sawers and L. H. Ting, "Perspectives on human-human sensorimotor interactions for the design of rehabilitation robots," *Journal of NeuroEngineering and Rehabilitation*, vol. 11, p. 142, Oct 2014.

[6] P. Morasso, M. Casadio, P. Giannoni, L. Masia, V. Sanguineti, V. Squeri, and E. Vergaro, "Desirable features of a "humanoid" robot-therapist," in *2009 Annual International Conference of the IEEE Engineering in Medicine and Biology Society*, pp. 2418–2421, Sep. 2009.

[7] R. Adolps, "Social cognition and the human brain," *Trends in Cognitive Sciences*, vol. 3, no. 12, p. 469–479, 1999.

[8] C. D. Frith and F. Uta, "Social cognition in humans," *Current Biology*, vol. 17, no. 16, pp. 724–732, 2007.

[9] P. Vuilleumier and G. Pourtois, "Distributed and interactive brain mechanisms during emotion face perception: Evidence from functional neuroimaging," *Neuropsychologia*, vol. 45, no. 1, pp. 174 – 194, 2007. The Perception of Emotion and Social Cues in Faces.

[10] C. D. Frith and U. Frith, "How we predict what other people are going to do," *Brain Research*, vol. 1079, no. 1, pp. 36 – 46, 2006. Multiple Perspectives on the Psychological and Neural Bases of Understanding Other People's Behavior.

[11] N. Jarrassé, T. Charalambous, and E. Burdet, "A framework to describe, analyze and generate interactive motor behaviors," *PLOS ONE*, vol. 7, pp. 1–13, 11 2012.

[12] K. B. Reed, M. Peshkin, M. J. Hartmann, J. Patton, P. M. Vishton, and M. Grabowecky, "Haptic cooperation between people, and between people and machines," in *2006 IEEE/RSJ International Conference on Intelligent Robots and Systems*, pp. 2109–2114, 2006.

[13] N. Beckers, *Haptic human-human interaction: motor learning & haptic communication*. PhD thesis, University of Twente, Netherlands, 7 2019.

[14] K. B. Reed and M. A. Peshkin, "Physical collaboration of human-human and human-robot teams," *IEEE Transactions on Haptics*, vol. 1, pp. 108–120, July 2008.

[15] G. Ganesh, A. Takagi, R. Osu, T. Yoshioka, M. Kawato, and E. Burdet, "Two is better than one: Physical interactions improve motor performance in humans," *Scientific Reports*, vol. 4, Jan 2014.

[16] C. Basdogan, C.-H. Ho, M. A. Srinivasan, and M. Slater, "An experimental study on the role of touch in shared virtual environments," *ACM Trans. Comput.-Hum. Interact.*, vol. 7, pp. 443–460, Dec. 2000.

[17] R. P. R. D. van der Wel, G. Knoblich, and N. Sebanz, "Let the force be with us: Dyads exploit haptic coupling for coordination," *Journal of Experimental Psychology: Human Perception and Performance*, vol. 37, no. 5, pp. 1420–1431, 2011.

[18] A. Takagi, G. Ganesh, T. Yoshioka, M. Kawato, and E. Burdet, "Physically interacting individuals estimate the partner's goal to enhance their movements," *Nature Human Behaviour*, vol. 1, Mar 2017.

[19] R. Hastie and T. Kameda, "The robust beauty of majority rules in group decisions," *Psychologocal Review*, vol. 112, no. 2, pp. 494–508, 2005.

[20] K. Kording and D. Wolpert, "Bayesian integration in sensorimotor learning," *Nature*, vol. 427, pp. 244–7, 02 2004.

[21] K. Mojtahedi, B. Whitsell, P. Artemiadis, and M. Santello, "Communication and inference of intended movement direction during human–human physical interaction," *Frontiers in Neurorobotics*, vol. 11, p. 21, 2017.

[22] L. Lundy-Ekman, *Neuroscience: Fundamentals for Rehabilitation.* St. Louis, Mo: Saunders/Elsevier, 4th ed., 2013.

[23] T. E. Milner, *Impedance Control*, pp. 1929–1934. Berlin, Heidelberg: Springer Berlin Heidelberg, 2009.

[24] D. Borzelli, B. Cesqui, D. J. Berger, E. Burdet, and A. D'Avella, "Muscle patterns underlying voluntary modulation of co-contraction.," *Plos One*, vol. 13, pp. 1–30, 2018.

[25] E. Burdet, R. Osu, D. Franklin, T. Milner, and M. Kawato, "The central nervous system stabilizes unstable dynamics by learning optimal impedance," *Nature*, vol. 414, Nov 2001.

[26] D. W. Franklin, R. Osu, E. Burdet, M. Kawato, and T. E. Milner, "Adaptation to stable and unstable dynamics achieved by combined impedance control and inverse dynamics model," *Journal of Neurophysiology*, vol. 90, no. 5, pp. 3270–3282, 2003.

[27] L. P. J. Selen, P. J. Beek, and J. H. van Diedrichsen, "Impedance is modulated to meet accuracy demands during goal-directed arm movements," *Experimental Brain Research*, vol. 172, pp. 129–138, Jun 2006.

[28] D. R. Lametti, G. Houle, and D. J. Ostry, "Control of movement variability and the regulation of limb impedance," *Journal of Neurophysiology*, pp. 3516–3524, 2007.

[29] R. Osu, N. Kamimura, H. Iwasaki, E. Nakano, C. M. Harris, Y. Wada, and M. Kawato, "Optimal impedance control for task achievement in the presence of signal-dependent noise," *Journal of Neurophysiology*, vol. 92, no. 2, pp. 1199–1215, 2004.

[30] Y. Ueyama and E. Miyashita, "Signal-dependent noise induces muscle co-contraction to achieve required movement accuracy: A simulation study with an optimal control," *Current Bioinformatics*, vol. 8, pp. 16–24, 02 2013.

[31] P. L Gribble, L. I Mullin, N. Cothros, and A. Mattar, "Role of cocontraction in arm movement accuracy," *Journal of neurophysiology*, vol. 89, pp. 2396–405, 06 2003.

[32] J. Heald, D. Franklin, and D. Wolpert, "Increasing muscle co-contraction speeds up internal model acquisition during dynamic motor learning," *Scientific reports*, vol. 8, no. 1, 2018.

[33] K. A. Thoroughman and R. Shadmehr, "Electromyographic correlates of learning an internal model of reaching movements," *Journal of Neuroscience*, vol. 19, no. 19, pp. 8573–8588, 1999.

[34] R. E. Kearney, R. B. Stein, and L. Parameswaran, "Identification of intrinsic and reflex contributions to human ankle stiffness dynamics," *IEEE Transactions on Biomedical Engineering*, vol. 44, pp. 493–504, June 1997.

[35] R. C. van't Veld, A. C. Schouten, H. van der Kooij, and E. H. F. van Asseldonk, "Validation of online intrinsic and reflexive joint impedance estimates using correlation with emg measurements," in *2018 7th IEEE International Conference on Biomedical Robotics and Biomechatronics (Biorob)*, pp. 13–18, Aug 2018.

[36] D. Ludvig and E. J. Perreault, "Estimation of joint impedance using short data segments," in *2011 Annual International Conference of the IEEE Engineering in Medicine and Biology Society*, pp. 4120–4123, 2011.

[37] E. Burdet, D. W. Franklin, and T. E. Milner, "Chapter 4 - single-joint neuromechanics," in *Human Robotics - Neuromechanics and Motor Control*, pp. 57 – 78, Mit Press Ltd, 1th ed., 2013.

[38] N. Hogan, "Adaptive control of mechanical impedance by coactivation of antagonist muscles," *IEEE Transactions on automatic control*, vol. 29, no. 8, 1984.

[39] N. Hogan, "The mechanics of multi-joint posture and movement control," *Biological Cybernetics*, vol. 52, pp. 315–331, Sep 1985.

[40] T. Milner, C. Cloutier, A. Leger, and D. Franklin, "Inability to activate muscles maximally during cocontraction and the effect on joint stiffness," *Experimental Brain Research*, vol. 107, no. 2, pp. 293–305, 1995.

[41] T. E. Milner and C. Cloutier, "Damping of the wrist joint during voluntary movement," *Experimental Brain Research*, vol. 122, pp. 309–317, Sep 1998.

Chapter 2

Thesis

The effect of partner performance on arm impedance modulation during haptic human-human interaction

E. Zwijgers

***Abstract*—Humans often coordinate movements with each other during haptic human-human interaction. Previous research showed that individual task performance improves when two partners are physically connected, but the underlying mechanisms of how we use haptic cues remain unclear. A study suggests that joint impedance might be a contributor of haptic communication during interaction. Joint impedance, changed by muscle co-contraction, is namely one of the strategies used by the neuromuscular system to generate accurate movements. This study investigated if the level of individual muscle co-contraction during haptic collaboration is related to the performance of one's partner during haptic human-human interaction. An experiment was developed in which participants haptically interacted through a compliant connection in a continuous tracking task. During the experiment, the amount of co-contraction was measured using electromyography sensors to determine muscle activity. The tracking performance of the participants was manipulated by applying visual noise to the target movement to obtain more pronounced performance differences between partners. Our results indicate that muscle co-contraction in the monoarticular shoulder muscles and partly in the monoarticular elbow muscles is modulated based on the performance of the partner. The amount of co-contraction was increased when haptically interacting with a worse partner compared to performing the task alone, while the amount of co-contraction was decreased when haptically interacting with a better partner. Besides, the co-contraction was negatively correlated with the performance of the partner when the interacting partner was better. Further research should reveal if the modulation of arm impedance is a genuine mechanism used to improve individual task performance during haptic human-human interaction.**

I. INTRODUCTION

Humans are talented in coordinating movements with one another during physical human-human interaction. Physical interaction requires partners to adapt, anticipate, and react to each other's forces and motions [1]. Parents, for instance, use haptic cues to teach their children how to walk. Likewise, a therapist can physically assist or motivate a patient during rehabilitation to retain motor functions after injury or disease. The latter has served as motivation for the design of intuitive and natural rehabilitation robots [2], [3]. A better understanding of haptic interaction between humans could enhance the design and control of such robots. However, the underlying mechanisms of how we use haptic human-human interaction to coordinate movements remain unclear.

Previous research showed that individual task performance improves when two partners are physically connected [4]–[6]. Reed and Peshkin [4] showed that the reaching time of participants decreased while being rigidly coupled to a partner. Ganesh et al. [5] performed an experiment in which participants tracked an unpredictably and continuously moving target while being compliantly coupled to a partner. They showed that physically interacting participants improved, regardless of whether the partner performance was better or worse than the individual's performance [5]. Takagi et al. [7], [8] explained the results of Ganesh et al. [5] by proposing that physically interacting partners continuously estimate each other's movement goal through the interaction force. The prediction of a participant's own target can be improved using the estimated goal of their partner. This theory assumes that accurate haptic communication has to occur in order to explain the performance benefits of haptic human-human interaction [6]. Although humans are reasonably accurate at discriminating two different forces in terms of magnitude, they show errors in force magnitude perception, especially when the forces are small [9]–[13]. Besides, humans cannot accurately estimate the precise direction of an applied force [10], [11]. Because of this, Beckers et al. [6] challenged the theory of Takagi et al. [7], [8] and showed that an accurate perception of the interaction force was not necessary to improve performance during haptic human-human interaction. This raises the question: what alternative mechanisms could be used to improve performance during haptic human-human interaction?

Mojtahedi et al. [14] showed that a partner ('follower') was able to infer the intended or imagined (but not executed) movement direction from the upper limb impedance of the other partner ('leader') while being rigidly coupled to one another. The follower was instructed to scan the workspace while the leader was instructed to stay within the centre of the workspace while preserving the intention to move in a given intended direction. This study suggests that joint impedance might be a contributor of haptic communication in haptic human-human interaction.

Several studies found that increasing joint impedance, both through co-contraction and reflex modulation, stabilises the limb to external force fields [15], [16]. Besides, a higher joint impedance suppresses the effects of internal noise on movement kinematics [17]. Joint impedance is therefore one of the strategies used by the neuromuscular system to generate accurate movements [17]–[21]. Besides, joint impedance is a mechanism used in the early phase of learning to accelerate the rate of dynamic motor learning [16], [22] and decreases as an internal model is formed [23]. Therefore, improvement of performance during haptic human-human interaction might be induced by adaptation of joint impedance.

Humans are able to control joint impedance through the modulation of muscle co-contraction [24]–[26]. During haptic human-human interaction, participants might change the amount of co-contraction based on the present interaction force. The amount of hinder or contribution of this force might cause participants to decrease their amount of co-contraction and let the interaction force guide them or increase their amount of co-contraction to resist the interaction force. In other words, participants could choose if they want to 'lead' or 'follow' their partner based on the amount of hinder or contribution of the interaction force and thus the individual performance of their partner. This study investigated if the level of muscle co-contraction during haptic collaboration is related to the performance of one's partner in haptic human-human interaction and could therefore be a mechanism used to induce improvement of performance.

An experiment was developed in which participants haptically interacted through a compliant connection in a continuous tracking task. During the experiment, the amount of co-contraction was measured using electromyography (EMG) sensors to determine muscle activity. The tracking performance of the participants was manipulated by applying visual noise to the target movement to obtain more pronounced performance differences between partners. We expected that the amount of muscle co-contraction of the participants was related to the performance of one's partner. Specifically, we expected that a participant interacting with a worse partner showed more co-contraction with respect to a subject interacting with a better partner since the interaction forces were more hindering. Besides, it is expected that a participant interacting with a worse partner will co-contract more with respect to no interaction and will therefore improve performance.

II. Materials and methods

Twenty-two participants (aged 19-29, 8 males and 14 females; all except two were right-handed according to the Edinburgh handedness inventory [27]) participated in the experiment. The study was designed following the principles of the Declaration of Helsinki and approved by the Ethical Committee of the University of Twente. All participants provided written informed consent and received compensation (gift card) for their participation regardless of their performance. The experiment lasted approximately one hour and a half.

The method is structured as follows: the fist section describes the robotic setup, followed by a section explaining the specific experimental task and design of visual noise. Thereafter the method to measure muscle activity is reported. The fourth section elaborates on the experimental design, including the structure of the experimental blocks and the protocol. Finally, the data analysis is discussed.

A. Robotic setup

The experiments were performed with a dual robotic setup consisting of two manipulanda as used in Beckers et al. [6] (see Fig 1). The manipulanda allowed arm movements in a circular planar workspace with a radius of 10 cm. The manipulanda were admittance-controlled such that the dynamics of the handle (a mass of 0.3 kg and a damping of $0.25\ \mathrm{N\,s\,m^{-1}}$) were the same across the complete workspace. Both participants had their own display which showed the circular workspace, the common target and their own cursor. Each cursor could be controlled by moving the handles of each manipulandum. The movement of the cursor and target were scaled to match the real-world movement. The forearm of the participants was supported in the gravity direction by a passive arm support at shoulder joint height, such that each participant's arm moved in a horizontal plane. The wrist joint of the participants was fixed with a brace (Thuasne Ligaflex Classic Open, size 1), immobilising the wrist joint, such that the participants could only move the handle through elbow and shoulder joint movement [16], [21], [28]. The brace was connected to the manipulandum handle at the center of the hand palm. The view of the partner and partner's display was obstructed by a curtain. Besides, a panel obstructed direct view of the arm and manipulandum of each participant. During the experiment, participants were not allowed to verbally communicate.

B. Task

The experiment consisted of a repeated planar tracking task in which the goal of the participants was to track the target as accurate as possible. The score, presented as the mean tracking error, and high score of each participant was shown after each trial. Both partners within a pair tracked the same continuously moving target during trials of 23 s followed by a 5 s break. The trajectory of the target (in cm) was defined as a sum of sines (see appendix B-B) [29]

$$\begin{aligned} x(t) &= 3.92\sin(1.57t+0.27)+3.46\sin(1.89t+0.50), \\ &\quad +2.68\sin(2.51t+3.89)+1.85\sin(3.46t-2.32), \\ y(t) &= 3.40\sin(1.89t-1.28)+2.99\sin(2.29t+3.76), \\ &\quad +2.32\sin(2.83t+9.93)+1.62\sin(3.77t+5.53). \end{aligned} \tag{1}$$

The target movement had a mean velocity of $12.04\ \mathrm{cm\,s^{-1}}$ with a maximum velocity of $20.14\ \mathrm{cm\,s^{-1}}$. An uniformly random start time for the signal was chosen ($t \in [t_0, t_0+20]s$) to prevent fast learning or other cognitive strategies [6].

1) Visual noise: The tracking performance of the participants was manipulated by applying visual noise to the target movement, similar to [30], [31]. The tracking error was linearly and significantly related to the amount of visual noise, such that greater visual noise resulted in larger tracking errors (see appendix A). The target was composed of a dynamic cloud around the actual target position (see Fig. 2). The dynamic cloud consisted of five circular spots that were displayed every millisecond. Each spot was regenerated, one at a time, every 500 ms by picking a new relative position and velocity with respect to the target (see Eq. A.1). The position and velocity parameters were determined from normal random distributions with a standard deviation of σ_p = 0.4 cm for the position, and from a set of five equally spaced values from σ_v

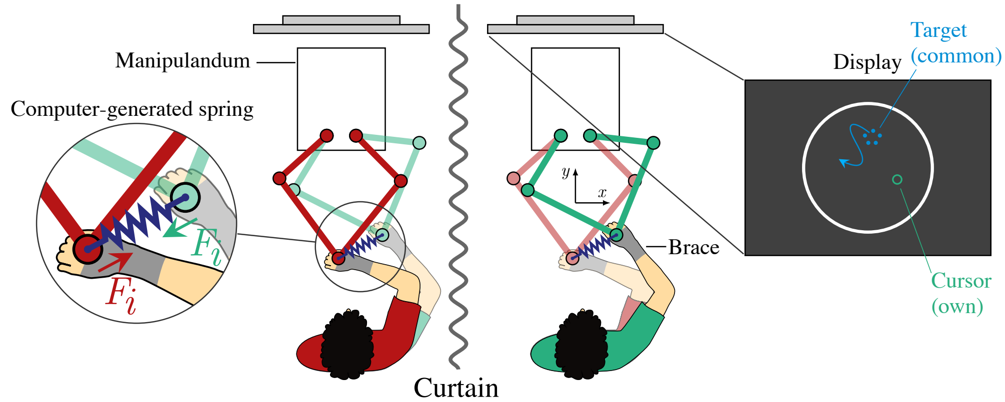

Fig. 1. Dual robotic setup. Each participant had his/her own manipulandum and display showing a cursor and target. The target was composed of a dynamic cloud around the trajectory consisting of five circular spots. The individual cursor could be controlled by moving the handle. The target movement was the same for both participants. The wrist joint of the participants was fixed by a brace which was connected to the handle of the manipulandum. The detail shows how the partners were physically coupled through a compliant computer-generated spring [6].

= 0.5 to σ_v = 10 cm s^{-1} for the velocity (see appendix B-A). The amount of visual noise was controlled by the standard deviation of the spots' velocities which was fixed during a trial. Spots with low velocity noise where relatively easy to track but high velocity noise spots spread out rapidly like fireworks.

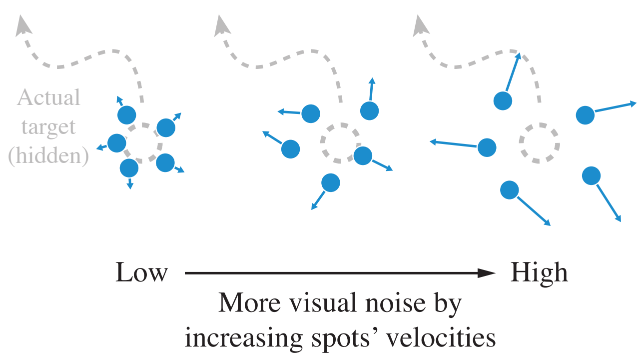

Fig. 2. The target was composed of a dynamic cloud around the actual target position. The dynamic cloud consisted of five circular spots which spread out slowly (low visual noise) or rapidly (high visual noise) to control each individual's tracking performance. The amount of visual noise was controlled by the amount of the standard deviation of the spots' velocities which was fixed during a trial [31].

2) Connected and single trials: Two types of trials were used in the experiment: *connected* (C) and *single* (S) trials. During a connected trial partners physically interacted through a compliant connection which connected the handles of the two partners (see Fig 1). The connection was a computer-generated spring, which generated an interaction force

$$\mathbf{F_s} = k_s(\mathbf{p_p} - \mathbf{p_o}) + b_s(\mathbf{v_p} - \mathbf{v_o}), \tag{2}$$

where k_s is the connection stiffness constant in N m^{-1}, b_s the damping constant in N s m^{-1}, $\mathbf{p_p}$ and $\mathbf{v_p}$ and $\mathbf{p_o}$ and $\mathbf{v_o}$ are the partner's and the participant's own position and velocity, respectively. The interaction force ($\mathbf{F_s}$) is exerted onto both partners' hands by the robotic manipulanda. The compliant connection allowed the partners to haptically interact, while being able to independently execute the tracking task such that independent and active task execution was required. The stiffness was set to k_s = 100 N m^{-1} [31] and the damping to b_s = 3 N s m^{-1}. The damping was added for spring stability. During a single trial, partners within a pair were not connected and performed the task alone.

C. Electromyography

We measured the muscle activity of three antagonistic muscle pairs through EMG using the Trigno™Avanti Wireless System (Delsys). The activity of two monoarticular shoulder muscles, pectoralis major and posterior deltoid, two biarticular muscles, biceps brachii and long head of the triceps, and two monoarticular elbow muscles, brachioradialis and lateral head of the triceps, were recorded [16], [32]. The electrode locations were chosen following the Seniam recommendations [33] to maximise the signal from a particular muscle while avoiding cross-talk from other muscles. Skin was prepared using alcohol and, if needed, removal of hair. Electrode placement was verified using isometric force tasks [21], [34].

D. Experiment design

The participants performed the experiment in randomly formed pairs (11 pairs). Each pair performed seven blocks of a various amount of trials, see Fig. 3A. Participants had a four-minute break between blocks. Block 1 consisted of one baseline trial to check the baseline level of EMG when participants were fully relaxed and eight maximal voluntary contraction (MVC) trials. MVC trials were performed by instructing the participants to maximally extend or flex the elbow or shoulder while static resistance was delivered by the experimenter. Block 2 served as a training block to achieve a steady-state behaviour. All trials in this block were single trials. The lowest visual noise level (σ_v = 0.5 cm s^{-1}) was applied to the first ten trials. In the following five trials the

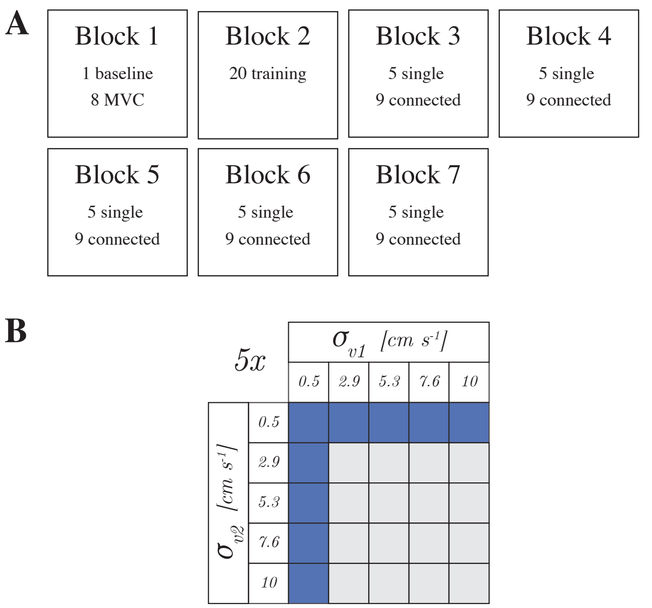

Fig. 3. The structure of the experimental blocks and the set of standard deviations of the velocity for both participants during connected trials. **A** The seven experimental blocks, including the amount and type of trials. The single and connected trials in block 3 to 7 were randomly ordered and randomly assigned with a standard deviation of the velocity. **B** The possible combinations for the standard deviation of the velocity for participant 1 (σ_{v1}) and participant 2 (σ_{v2}), denoted by the purple boxes. Each of the nine combinations is repeated five times (45 connected trials in total).

visual noise level was increased in ascending order. In the last five trials the five levels of visual noise were applied randomly to get the participants acquainted with randomly changing visual noise levels.

Block 3 to 7 consisted of five single and nine connected trials, which were randomly presented to the partners. In these blocks, at the start of each connected trial one of the levels of visual noise was assigned to each of the participants. One of the two participants was always assigned with a visual noise level with a standard deviation of 0.5 $\mathrm{cm\,s^{-1}}$ while the other participant got a visual noise level with a standard deviation from the set of five equally spaced values, see Fig. 3B. Every combination of visual noises for the connected trials (total of nine) was applied only once within a block. During the five single trials within each block, a level of visual noise was randomly assigned for both participants separately and only applied once per block.

E. Analysis

Data of the handle position and velocity, interaction force and EMG signals were sampled at 1 kHz. The data were then parsed to perform additional analysis using MATLAB R2017B. Individual performance was calculated as the root mean square of the tracking error E (in cm) and only the last 20 s of each trial was used. The tracking error is referred to E_s in a single trial and E_c in a connected trial. EMG data were high-pass filtered using a 30 Hz cut-off frequency to remove ECG cross-talk and movement artefacts [35]. The signal was then rectified and filtered using a moving average filter with a window of 0.5 s for the baseline and MVC trials and a window of 0.3 s for all other trials [36]. The MVC value for each muscle is defined as the highest peak in the corresponding MVC trial. EMG data of every muscle were scaled using the MVC value of the specific muscle.

1) Improvement of performance due to interaction: The improvement of performance due to interaction with a partner is visualised using the relative performance between partners and performance improvement due to interaction [5]–[7]. The performance improvement per participant due to interaction (*I*) is calculated as

$$I = 1 - \frac{E_c}{E_s}, \tag{3}$$

where the error of the connected trial (E_c) is compared to the error of the single trial (E_s) with the equivalent level of visual noise in the same experimental block. The relative performance of the partner (*R*) you interact with is calculated as

$$R = 1 - \frac{E_{s,p}}{E_s}, \tag{4}$$

where $E_{s,p}$ is the partner's performance during the single trial in which the level of visual noise was the same as the level of visual noise of the partner in the connected trial and belongs to the same experimental block. The improvement is binned in bins of 20% of relative performance wide to reveal any trend in the improvement *I* versus relative performance *R*. The mean and standard error of the mean (s.e.m.) of the improvement were calculated per bin.

2) Co-contraction index: To investigate how muscle co-contraction during interaction dependeds on the performance of the partner, the absolute difference in performance between partners and the level of co-contraction for the three antagonistic muscle pairs is determined. The level of co-contraction (co-contraction index, *CI*) in each trial is calculated as (see Appendix C) [37]–[39]

$$CI = \sqrt{\frac{1}{n}\sum_{i=1}^{n}(\text{common area muscle } A \text{ \& } B)^2}, \tag{5}$$

where muscle *A* and *B* represent the antagonistic muscles. The co-contraction index in connected trials is compared against the absolute difference of performance of the two partners (ΔR) and is calculated as

$$\Delta R = E_s - E_{s,p}. \tag{6}$$

3) Statistical analysis: Statistical analysis was done using IBM SPSS Statistics 25. The improvement due to interaction versus relative partner performance was fitted using an exponential regression model

$$I_{i,j} = \alpha_0 + \alpha_1 e^{\alpha_2 R_{i,j}} + \epsilon_{i,j}, \tag{7}$$

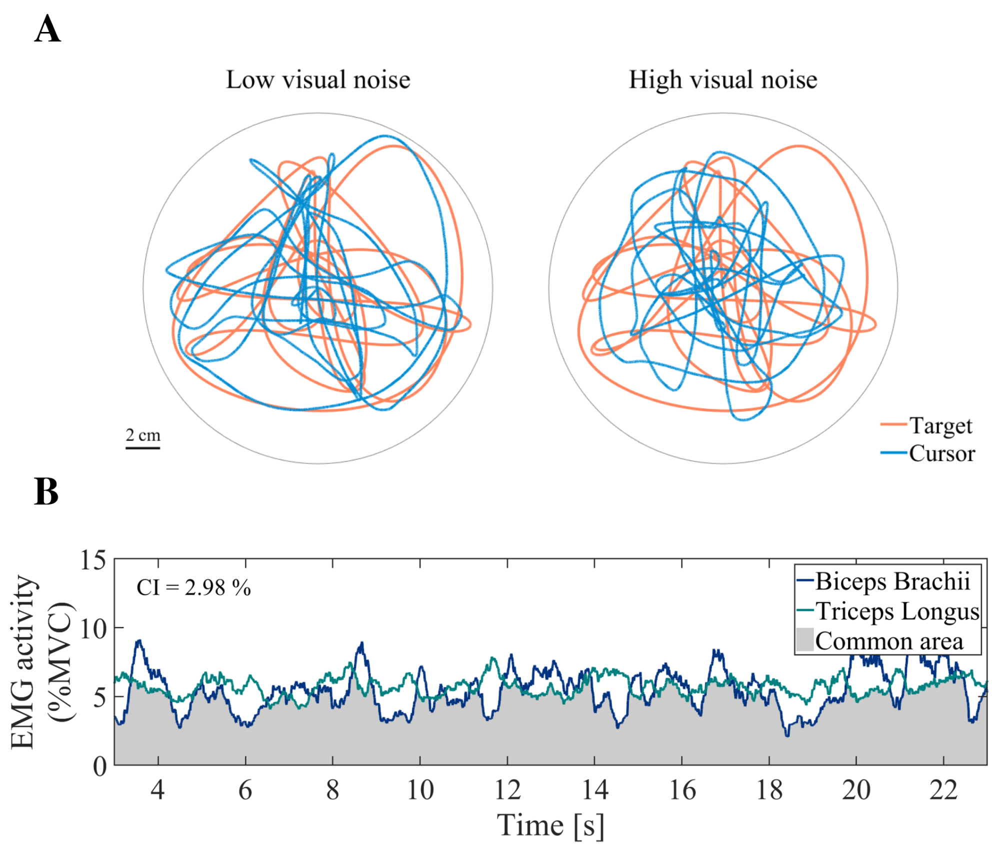

Fig. 4. Example of participant's cursor path and muscle activity measured with EMG. **A** The cursor and target path of a participant during single trials. A trial with low visual noise ($\sigma_v = 0.5$ cm s^{-1}) and high visual noise ($\sigma_v = 10$ cm s^{-1}) is shown. **B** EMG activity normalised with the maximal voluntary contraction (MVC) of the biarticular muscles (biceps brachii and long head of the triceps) for a random trial. The shaded area denotes the common area of the antagonistic muscle pair. The co-contraction index (CI) is calculated as the root mean square of the common area.

where R is the relative partner performance (continuous predictor), $\alpha_{0...2}$ the fitted coefficients, ϵ is the unexplained variance in the data and the subscript i and j denote the trial number and participant, respectively. Where applicable, parametric statistical tests (ANOVA and repeated measures ANOVA) were used to analyse the effect of visual noise on the individual performance and co-contraction index. The co-contraction index of the three antagonistic muscle pairs during interaction versus the absolute difference in performance of the two partners were analysed using a linear mixed model with a random intercept and fixed slope [40]

$$CI_{i,j} = \beta_{0_j} + \beta_1 \Delta R_{i,j} + \epsilon_{i,j} \tag{8}$$

where β_{0_i} and β_1 are the random intercept and fixed slope, respectively, ΔR the absolute difference in partner performance, ϵ is the unexplained variance in the data and the subscripts i and j denote the trial number and subject, respectively. All data and statistical model fit residuals were checked for normality using the Kolmogorov-Smirnov normality test and visual inspection (QQ plots). In case of non-normality, the non-parametric Friedman's ANOVA is used for K-related samples with the Wilcoxon signed-rank test as post hoc analysis using a Bonferroni correction to account for multiple testing bias. For the regression model and linear mixed model, in case of non-normality of the residuals, the robust bootstrap method is used for analysis [41], [42]. A two-tailed dependent t-test or a two-tailed Wilcoxon signed-rank test, in case of non-normality, is performed to see if the amount of co-contraction significantly differed between interaction and no interaction. The level of significance for all tests was set to 0.05 unless specifically mentioned differently.

III. Results

To investigate how relative partner performance influenced arm impedance modulation during haptic human-human interaction, a collaborative tracking task was performed. The performance of participants was manipulated using visual noise to obtain more pronounced performance differences between partners. Muscle activity of six upper limb muscles was measured to assess participants' adopted levels of muscle co-contraction. The first section will discuss the results on the improvement of the tracking performance due to haptic human-human interaction and if this is influenced by adding visual noise to the target. Thereafter, we discuss whether

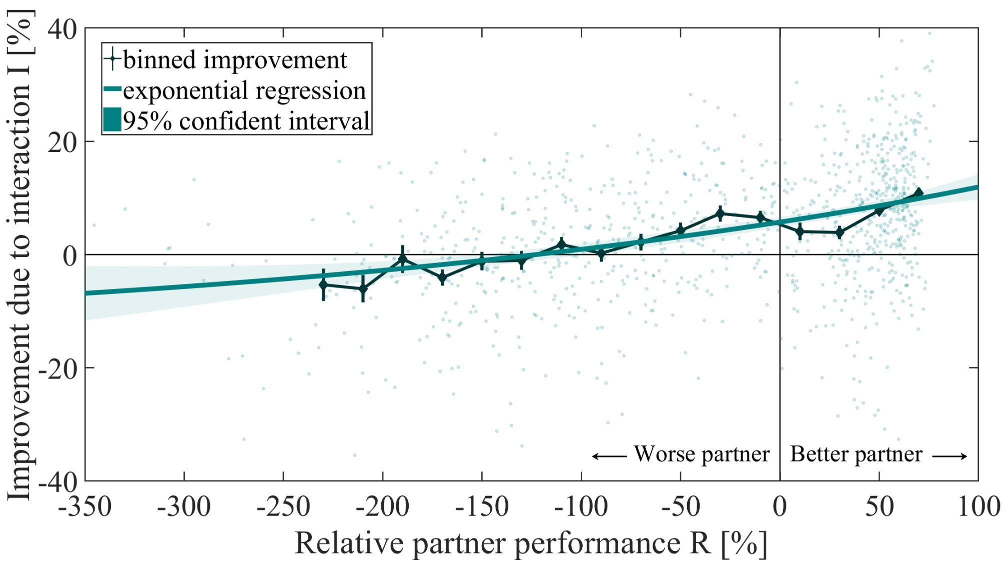

Fig. 5. The improvement in task performance in each participant for each dual trial was plotted against the relative performance of their partner. Improvement is observed when the partner is better and partly when the partner is worse, up till a relative partner performance of ± -120%.

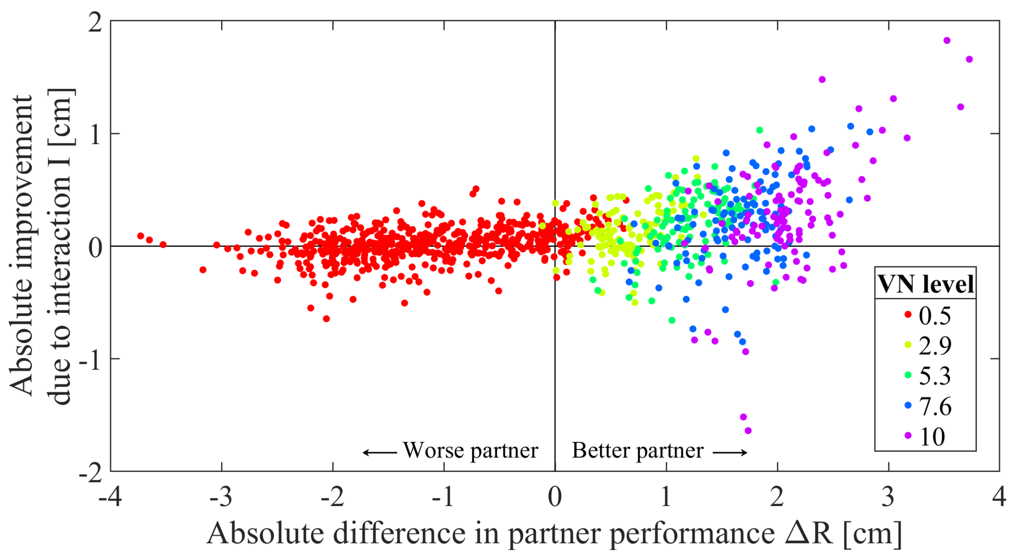

Fig. 6. The absolute improvement in task performance in each participant for each dual trial was plotted against the absolute difference performance in partner performance and grouped per level of visual noise. The spread in absolute improvement increased with a higher level of visual noise (VN).

muscle co-contraction is modulated based on the performance of the partner.

A. Improvement due to interaction

Fig. 4A shows an example of the cursor paths of one participant when a low and high level of visual noise was added to the target. The tracking performance with a low level of visual noise was much better compared to the tracking performance with a high level of visual noise.

To analyse how each individual's performance changed as a function of the partner's performance during haptic human-human interaction in a connected trial, the relative improvement due to interaction as a function of the relative partner performance is plotted in Fig. 5. The data was fitted using an exponential regression model ($R^2 = 0.17$), with the relative partner performance as a significant predictor ($t(979) = 11.99$, $p = 5.35 \cdot 10^{-31}$). The performance of a participant improved when the interacting partner was better. Moreover, the improvement increased as the performance of the partner increased. Participants still improved when their partner was worse then them, but improvement benefits decreased towards zero with a progressively worse partner. The improvement due to haptic human-human interaction is similar to those of Ganesh et al. [5] and Beckers et al. [6], but there is a main difference in the interception point (i.e. where the improvement is zero). The data of Ganesh et al. suggest that you will improve regardless of the performance of the partner. The

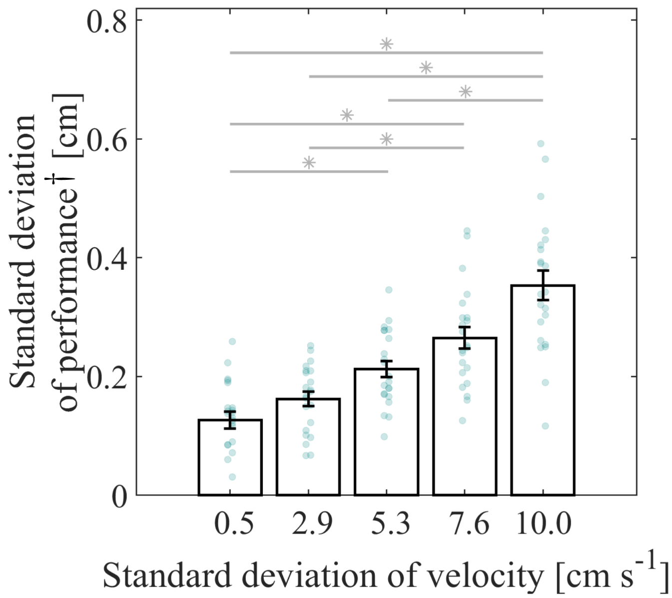

Fig. 7. The standard deviation of the performance in single trials is plotted against the level of visual noise. The green data points represent an individual participant. The variability between a certain visual noise level and the not immediately adjacent visual noise levels differ significantly, $p < 0.05$. † To account for individual differences, the standard deviation (σ) was adjusted: $\sigma_{adjusted_{i,p}} = \sigma_{i,p} + (\frac{1}{P}\sum_{p=1}^{P}\overline{\sigma}_g - \frac{1}{N}\sum_{i=1}^{N}\sigma_{i,p})$, where n and p denote the trial number and participant number, respectively, and $\overline{\sigma}_g$ denotes the mean standard deviation of each participant.

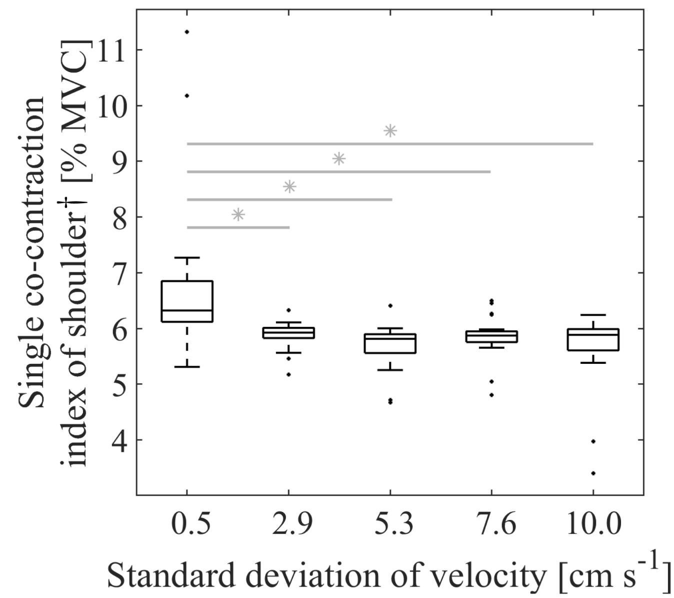

Fig. 8. The co-contraction index of the shoulder antagonistic muscle pair in single trials is plotted against the level of visual noise. The first level of visual noise (0.5 cm s^{-1}) significantly differed from the other levels of visual noise, $p < 0.05$. † To account for individual differences, the co-contraction index (CI) was adjusted: $CI_{adjusted_{i,p}} = CI_{i,p} + (\frac{1}{P}\sum_{p=1}^{P}\overline{CI}_g - \frac{1}{N}\sum_{i=1}^{N}CI_{i,p})$, where n and p denote the trial number and participant number, respectively, and $\overline{CI}_g$ denotes the mean co-contraction index of each participant.

data of Beckers et al. show an intercept of approximately -40% while this data suggests an intercept of approximately -120%. Besides, our data show less improvement of performance when connected to a partner with the same performance compared to the study of Ganesh et al. and Beckers et al. In addition, our data show more data points in the lower-right quadrant (indicating deterioration of performance with a better partner) compared to the data of Ganesh et al. and Beckers et al. To investigate this difference, the absolute improvement due to interaction as a function of the absolute difference in partner performance, grouped per level of visual noise, is plotted in Fig. 6. The spread in absolute improvement increased with higher levels of visual noise. To further investigate the effect of visual noise on the variability in performance, the standard deviation of the performance per level of visual noise in single trials is shown in Fig. 7. A repeated measures ANOVA showed that the magnitude of standard deviation of the performance was significantly affected by the amount of visual noise ($F(2.62, 54.92) = 21.71$, $p = 8.73 \cdot 10^{-9}$; Mauchly's test showed violation of sphericity, $\chi^2(9) = 22.47$, $p = 0.008$, Greenhouse-Geisser correction is therefore applied). Post hoc tests using the Bonferroni correction showed that the standard deviation of the performance was significantly different for all combinations of visual noise except the adjacent pairs of visual noise, $p < 0.05$. The variability in performance thus increased with a higher level of visual noise. The higher amount of data points for deterioration of performance when coupled to a better partner is most likely due to a higher variability in performance with a higher level of visual noise.

B. Co-contraction modulation due to partner performance

Fig. 4B shows the measured EMG activity and the inferred muscle co-contraction of the biarticular muscle pair for one participant within one single trial.

1) Effect of visual noise on co-contraction: Before we could analyse the effect of partner performance on the amount of co-contraction during the connected trials, we needed to analyse the effect of visual noise on the amount of co-contraction in the single trials. This is done to ensure that an effect on the amount of co-contraction is due to partner performance and not visual noise. Fig. 8 shows the co-contraction index in single trials per level of visual noise for the monoarticular shoulder muscles. We found that there was a significant effect of the level of visual noise on the amount of co-contraction in single trials (Friedman's ANOVA non-parametric tests; $\chi^2(4) = 38.84$, $p = 7.53 \cdot 10^{-8}$; $\chi^2(4) = 22.22$, $p = 1.81 \cdot 10^{-5}$; $\chi^2(4) = 26.66$, $p = 2.30 \cdot 10^{-6}$, for the monoarticular elbow muscles, monoarticular shoulder muscles and biarticular muscles, respectively). Wilcoxon signed-rank tests were used to follow up this finding and a Bonferroni correction was applied. It appeared that only the amount of co-contraction in the lowest level of visual noise (0.5 cm s^{-1}) significantly differed from the other levels of visual noise for all three antagonistic muscle pairs ($p < 0.005$).

2) Relation between partner performance and co-contraction: Because there was a significant effect between

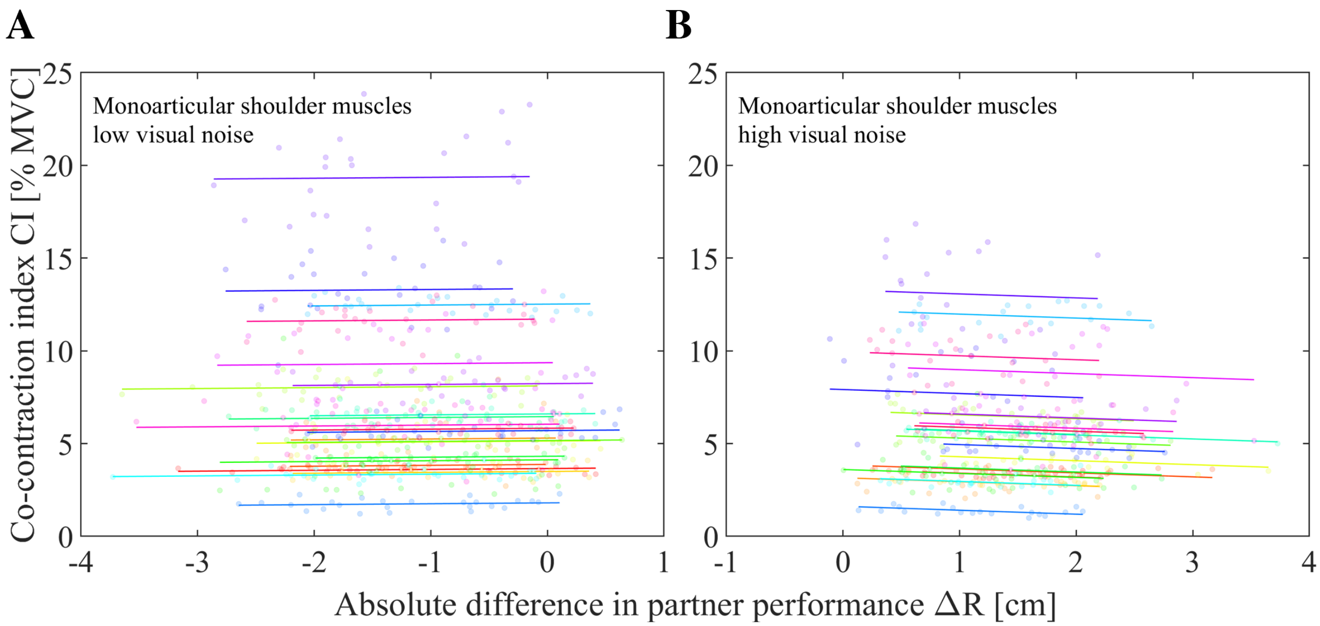

Fig. 9. The co-contraction index of the monoarticular shoulder muscles during interaction as a function of the absolute difference in partner performance. Each color represents a specific participant. Data points are fitted using a linear mixed model with a random intercept and fixed slope. **A** Data points are measured when a low level of visual noise was applied to the target ($\sigma_v = 0.5$ cm s^{-1}). **B** Data points are measured when a high level of visual noise was applied to the target ($\sigma_v = 2.9$, 5.3, 7.6, 10 cm s^{-1}).

the level of visual noise and the amount of co-contraction, visual noise was taken into account when analysing the effect of the performance of one's partner on the amount of co-contraction. The level of visual noise and the absolute difference in partner performance are strongly subjected to multicollinearity (Pearson correlation test; $r = 0.815$, $p = 9.98 \cdot 10^{-12}$) and it was therefore not possible to include visual noise as a covariate in the linear mixed model (see Eq. 8). We therefore chose to split the data of the monoarticular elbow muscles, monoarticular shoulder muscles and the biarticular muscles in two groups based on the level of visual noise. The first group, labelled as *low visual noise*, consisted of all trials with the lowest level of visual noise ($\sigma_v = 0.5$ cm s^{-1}). The second group, labelled as *high visual noise*, consisted of trials with all other levels of visual noise ($\sigma_v = 2.9$, 5.3, 7.6, 10 cm s^{-1}). Fig. 9A and 9B show the co-contraction index of the monoarticular shoulder muscles in connected trials as a function of the absolute difference in partner performance for the low visual noise group and high visual noise group, respectively (see appendix E for figures of monoarticular elbow muscles and biarticular muscles). Using the linear mixed model (see Eq. 8), the absolute difference in partner performance significantly predicted the co-contraction index of the monoarticular elbow muscles and monoarticular shoulder muscles for a high level of visual noise, $F(1, 418.34) = 7.50$, $p = 0.006$ and $F(1, 418.62) = 9.82$, $p = 0.002$, respectively. The relation between the absolute difference in partner performance and the co-contraction index is negative and has a slope of $\beta_1 = -0.15$ and $\beta_1 = -0.21$ $\frac{\%MVC}{cm}$ for the monoarticular elbow muscles and monoarticular shoulder muscles, respectively. The absolute difference in partner performance did not significantly predicted the co-contraction index of the biarticular muscles for a high level of visual noise ($F(1, 418.47) = 2.30$, $p = 0.13$) and for all three antagonistic muscle pairs for the low level of visual noise, $F(1, 528.25) = 1.95$, $p = 0.16$; $F(1, 528.28) = 0.26$, $p = 0.61$; $F(1, 528.29) = 1.03$, $p = 0.31$, for the monoarticular elbow muscles, monoarticular shoulder muscles and biarticular muscles, respectively.

3) Effect of interaction on co-contraction: Fig. 10 shows the average amount of co-contraction for the monoarticular shoulder muscles, monoarticular elbow muscles and biarticular muscles during trials without haptic interaction and during trials with haptic interaction for a low and high level of visual noise. The amount of co-contraction of the monoarticular shoulder muscles during haptic interaction with a low level of visual noise significantly increased with respect to no haptic interaction (two-tailed Wilcoxon signed-rank tests; $z = -2.64$, $p = 0.008$). A change in co-contraction with a low level of visual noise was not seen in the monoarticular elbow and biarticular muscles, $z = -0.21$, $p = 0.83$; $z = -0.50$, $p = 0.61$, respectively. The amount of co-contraction during haptic interaction significantly decreased with respect to no haptic interaction with a high level visual noise, for the monoarticular shoulder muscles (two-tailed Wilcoxon signed-rank tests; $z = -2.52$, $p = 0.012$). A change in co-contraction with a high level of visual noise was not seen in the monoarticular elbow and biarticular muscles, $z = -0.016$, $p = 0.99$; $z = -0.89$, $p = 0.37$, respectively.

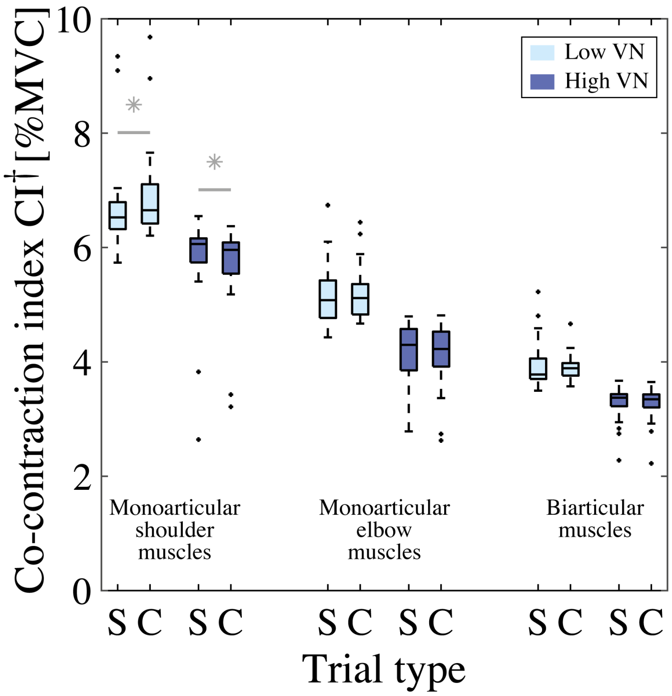

Fig. 10. The average co-contraction index of the monoarticular shoulder muscles, monoarticular elbow muscles and biarticular muscles with a low and high level of visual noise (VN). The average co-contraction indexes are plotted for single (S) trials in which participants were not haptically connected and for connected (C) trials in which participants were haptically connected to one another. The average co-contraction index in the monoarticular shoulder muscles in connected trials differed significantly from the single trials in both the low visual noise and high visual noise group. † To account for individual differences, the co-contraction index (CI) for all three muscle groups separately was adjusted: $CI_{adjusted_{i,p}} = CI_{i,p} + (\frac{1}{P}\sum_{p=1}^{P}\overline{CI}_g - \frac{1}{N}\sum_{i=1}^{N} CI_{i,p})$, where n and p denote the trial number and participant number, respectively, and $\overline{CI}_g$ denotes the mean co-contraction index of each participant.

4) Relation between visual noise and performance of the partner: The level of visual noise was directly related to the absolute difference in partner performance, such that a low level of visual noise ($\sigma_v = 0.5$ cm s^{-1}) resulted almost always in a worse partner (89.6 %) and a high level of visual noise ($\sigma_v > 0.5$ cm s^{-1}) resulted almost always in a better partner (99.5%). It can therefore be said that the results obtained within the low level of visual noise group say something about a worse partner performance and the results obtained within the high level of visual noise group say something about a better partner performance.

IV. Discussion

This study investigated if muscle co-contraction - an indicator of arm impedance - during haptic collaboration is related to the performance of one's partner during haptic human-human interaction. Participants tracked a common randomly moving target while haptically interacting though a compliant connection. The tracking performance of the participants was manipulated by using visual noise to obtain more pronounced performance differences between partners. Visual noise was created by representing the target as a cloud of randomly moving dots which spread out slowly (low visual noise) or rapidly (high visual noise). The muscle activity of six upper limb muscles was measured using EMG to assess each participant's adopted levels of muscle co-contraction. First, the relation between co-contraction and the performance of the partner is discussed. Thereafter, we discuss the effect of visual noise on the improvement due to interaction and the variability in performance. Finally, we describe the limitations of this study and suggestions for further research.

A. Co-contraction modulation due to partner performance

Our results show that muscle co-contraction was changed based on the performance of the partner. The co-contraction in the monoarticular shoulder muscles (pectoralis major and posterior deltoid) was increased during interaction with a worse partner compared to performing the task alone. Furthermore, the co-contraction in the monoarticular shoulder muscles was decreased when being connected to a better partner compared to no interaction, and gradually decreased with increasing partner performance. The co-contraction in the monoarticular elbow muscles (brachioradialis and lateral head the triceps) was not significantly different when being connected to a better partner compared to no interaction. Yet, there was a negative correlation between the co-contraction and the performance of the partner when the interacting partner was better. No change in co-contraction in the monoarticular elbow muscles was found when being connected to a worse partner. The co-contraction in the biarticular muscles (biceps brachii and long head of the triceps) did not change based on the performance of the partner. This study thus provides evidence that haptically interacting partners modulate co-contraction of the monoarticular shoulder muscles and partly the monoarticular elbow muscles based on their partner's performance, which indicates that the individuals selected different arm impedance modulation strategies based on their partner's performance.

1) Co-contraction strategies: Our results show that the co-contraction in the elbow and shoulder muscles is modulated independently, which is supported by the findings of Gribble and Ostry [43]. They found that humans modulate co-contraction in the shoulder and elbow independently based on task requirements during arm reaching movements. Moreover, Franklin et al. [44] showed that co-contraction of the different muscle groups in the shoulder and elbow joints was selectively controlled when moving in differently orientated unstable environments. This indicates that the central nervous system (CNS) selectively changes the co-contraction of muscle groups and thus applies different strategies depending on the environment and task requirements. The application of different strategies is also seen in our study as co-contraction increases when the partner's performance is worse and decreases as the partner's performance is better.

The geometry of the arm has an influence on the contribution of particular muscles on the endpoint stiffness [44]. For example, when the arm is relatively extended in front of the body, an increase in the arm impedance in the x-

direction can only be achieved by increasing the co-contraction of the monoarticular shoulder muscles. When the arm is more flexed, a similar increase in arm impedance can be produced by either the monoarticular shoulder muscles, the biarticular muscles or the monoarticular elbow muscles. An increase in co-contraction in the monoarticular shoulder muscles is effective in most arm geometries and might therefore be the preferred method of the CNS to modulate arm impedance during a tracking task in haptic human-human interaction.

2) Increased co-contraction when interacting with a worse partner: The co-contraction in the monoarticular shoulder muscles was increased when being connected to a worse partner compared to the co-contraction levels when performing the task alone. To explain this finding, it is possible that participants interacting with a worse partner perceived the interaction force as a perturbation and increased their co-contraction in order to be more robust to (unanticipated) external interaction forces [15], [16]. In addition, several studies have shown that a higher arm impedance causes higher movement accuracy [17]–[21]. Hence, the increased arm impedance during interaction with a worse partner (up till a relative partner performance of -120%) could have resulted in better or at least no degraded tracking performance. When the performance of the partner was worse than approximately 120%, the interaction force was presumably more hindering than providing accuracy benefits, due to increased co-contraction, resulting in deterioration of performance during interaction.

3) Decreased co-contraction when interacting with a better partner: The co-contraction in the monoarticular shoulder muscles was decreased when being connected to a better partner compared to performing the task alone. Besides, the co-contraction in the monoarticular shoulder and elbow muscles was negatively correlated with the performance of the partner when the interacting partner was better. Previous studies suggest that the CNS attempts to decrease levels of muscle activation - referred to as slacking - when haptically assisted [45]–[49]. During haptic assistance, participants rely on the external help as movement errors remain small. Our results could indicate that participants were slacking when connected to a better partner as they relied on the haptic guidance provided by their partner to improve performance. Besides, participants seemed to slack more, or rely more on the haptic guidance provided by their partner when their partner became even better (based on the decreased co-contraction levels), presumably because a better partner caused smaller movement errors when being followed.

B. Effect of visual noise on improvement

We found that the amount of co-contraction increased when the target with the lowest level of visual noise was presented ($\sigma_v = 0.5$ cm s^{-1}) compared to all other levels of visual noise. Previous studies have shown that muscle co-contraction voluntarily increases with increasing accuracy requirements, leading to reduced endpoint deviations in reaching tasks [21], [50], [51]. Participants had the highest chance to improve their high score (shown after each trial) in trials with the lowest level of visual noise. Because humans have a competitive nature [52] they likely increased their muscle co-contraction in order to increase movement accuracy and therefore try to improve their high score. This matches the opinion of the participants. Most participants stated that they were more motivated when the lowest level of visual noise was presented.

The effect of increased muscle co-contraction with the lowest level of visual noise on the improvement due to interaction is visible when comparing this study to the study of Beckers et al. [6]. We found lower improvement when connected to a partner with the same performance and participants still improved with a relatively worse partner. This is due to the fact that participants with the lowest level of visual noise performed better without interaction and were more stabilised to the interaction force [15], [16]. Less improvement of performance due to visual noise was also seen in the results of Takagi et al. [31] who also introduced visual noise to the target.

C. Effect of visual noise on variability

The visual noise on the target made accurate estimation of the target position more difficult [30] and subsequently led to lower accuracy when tracking the target, resulting in a worse performance. Moreover, the results of this study show that the variability of performance increased with greater visual noise. Visual noise therefore introduces, alongside lower accuracy, lower precision. This is in accordance to the study of Ma-Wyatt and McKee [53] who studied the endpoint precision for a rapid pointing task when the amount of visual information was adjusted. Similar to this study, Takagi et al. [31] performed a continuous tracking task with physically coupled dyads, triads and tetrads from which their tracking performance was manipulated by adding visual noise similar to us. A high variability in performance due to visual noise is, however, not seen in the study of Takagi et al. The difference can be explained by a methodological difference since the tracking error during no interaction is determined differently compared to this study. The method of Takagi is disregarding a higher variability in performance due to visual noise while it should be taken into account when analysing performance.

D. Limitations

1) Effect of visual noise on co-contraction: A relation between the partner performance and the amount of co-contraction in the monoarticular shoulder muscles when the partner performance was worse was not found. Yet, the amount of co-contraction did increase in the monoarticular shoulder muscles when connected to a worse partner compared to no interaction. The absence of a trend can be assigned to an increased amount of co-contraction without interaction due to a low level of visual noise. Since participants are already more co-contracted when doing the task alone, they might not increase their amount of co-contraction much more during interaction. Muscle co-contraction is namely metabolically expensive, and thus with respect to energetic considerations alone, would not represent an optimal strategy for movement control [54]. However, in order to stabilise the limb to external forces, the optimal compromise between energy consumption and accuracy does in fact require antagonistic muscle activation [55]. During connection with a slightly worse partner the maximum compromise in favour of co-contraction might already be achieved and thus not further increase during interaction with a much worse partner. The introduction of visual noise resulted in more pronounced differences in performance but possibly obscured the relation between muscle co-contraction and a worse partner performance.

2) Co-contraction measuring method: The measure of co-contraction used in this study has a few limitations. The co-contraction index is solely based on surface EMG signals and thus does not take into account factors such as differences in the muscle force-generating ability or differences in muscle moment arms [21]. Besides, muscles not monitored in this study could also have a contribution to the impedance of the upper limb. Moreover, the EMG activity of all six muscles was relatively low (average maximum of 20 %MVC) which could cause a low signal to noise ratio. Nevertheless, as a first approximation, the measure used here is useful as a rough estimate of how opposing agonist/antagonist activity during interaction changes with respect to partner performance. Besides, other methods to measure co-contraction are not suitable during haptic human-human interaction experiments since the interaction force would disturb these measurements (see Appendix C).

E. Further research

This study only looked at the modulation of co-contraction per trial, but it is interesting to see how co-contraction is changed within a trial and if it is modulated based on the amplitude and direction of the haptic interaction force. It is recommended for further research to investigate the direct relation between co-contraction and the interaction force.

Our results indicate that muscle co-contraction in the monoarticular shoulder muscles and partly in the monoarticular elbow muscles is modulated based on the performance of the partner. We found a connection between arm impedance modulation and improvement during interaction; however, it is possible that haptically-interacting partners improved performance through other strategies as well. Further research should reveal if the modulation of arm impedance is a genuine mechanism used to improve individual task performance during haptic human-human interaction.

References

[1] K. B. Reed, M. Peshkin, M. J. Hartmann, J. Patton, P. M. Vishton, and M. Grabowecky, "Haptic cooperation between people, and between people and machines," in *2006 IEEE/RSJ International Conference on Intelligent Robots and Systems*, 2006, pp. 2109–2114.

[2] A. Sawers and L. H. Ting, "Perspectives on human-human sensorimotor interactions for the design of rehabilitation robots," *Journal of NeuroEngineering and Rehabilitation*, vol. 11, no. 1, p. 142, Oct 2014.

[3] N. Jarrassé, T. Charalambous, and E. Burdet, "A framework to describe, analyze and generate interactive motor behaviors," *PLOS ONE*, vol. 7, no. 11, pp. 1–13, 11 2012. [Online]. Available: https://doi.org/10.1371/journal.pone.0049945

[4] K. B. Reed and M. A. Peshkin, "Physical collaboration of human-human and human-robot teams," *IEEE Transactions on Haptics*, vol. 1, no. 2, pp. 108–120, July 2008.

[5] G. Ganesh, A. Takagi, R. Osu, T. Yoshioka, M. Kawato, and E. Burdet, "Two is better than one: Physical interactions improve motor performance in humans," *Scientific Reports*, vol. 4, no. 3824, Jan 2014.

[6] N. Beckers, "Haptic human-human interaction: motor learning & haptic communication," Ph.D. dissertation, University of Twente, Netherlands, 7 2019.

[7] A. Takagi, G. Ganesh, T. Yoshioka, M. Kawato, and E. Burdet, "Physically interacting individuals estimate the partner's goal to enhance their movements," *Nature Human Behaviour*, vol. 1, no. 54, Mar 2017.

[8] A. Takagi, F. Usai, G. Ganesh, V. Sanguineti, and E. Burdet, "Haptic communication between humans is tuned by the hard or soft mechanics of interaction," *PLOS Computational Biology*, vol. 14, no. 3, pp. 1–17, 03 2018.

[9] L. A. Jones, "Matching forces: Constant errors and differential thresholds," *Perception*, vol. 18, no. 5, pp. 681–687, 1989.

[10] F. E. van Beek, W. M. B. Tiest, and A. M. L. Kappers, "Anisotropy in the haptic perception of force direction and magnitude," *IEEE Transactions on Haptics*, vol. 6, pp. 399–407, 2013.

[11] F. Beek, W. M. Bergmann Tiest, W. Mugge, and A. M. L. Kappers, "Haptic perception of force magnitude and its relation to postural arm dynamics in 3d," *Scientific Reports*, vol. 5, p. 18004, 12 2015.

[12] B. Onneweer, W. Mugge, and A. C. Schouten, "Force reproduction error depends on force level, whereas the position reproduction error does not," *IEEE Transactions on Haptics*, vol. 9, no. 1, pp. 54–61, Jan 2016.

[13] N. Gurari, A. M. Okamura, and K. J. Kuchenbecker, "Perception of force and stiffness in the presence of low-frequency haptic noise," *PLOS ONE*, vol. 12, no. 6, pp. 1–26, 06 2017.

[14] K. Mojtahedi, B. Whitsell, P. Artemiadis, and M. Santello, "Communication and inference of intended movement direction during human–human physical interaction," *Frontiers in Neurorobotics*, vol. 11, p. 21, 2017.

[15] E. Burdet, R. Osu, D. Franklin, T. Milner, and M. Kawato, "The central nervous system stabilizes unstable dynamics by learning optimal impedance," *Nature*, vol. 414, no. 446, Nov 2001.

[16] D. W. Franklin, R. Osu, E. Burdet, M. Kawato, and T. E. Milner, "Adaptation to stable and unstable dynamics achieved by combined impedance control and inverse dynamics model," *Journal of Neurophysiology*, vol. 90, no. 5, pp. 3270–3282, 2003.

[17] L. P. J. Selen, P. J. Beek, and J. H. van Diedrichsen, "Impedance is modulated to meet accuracy demands during goal-directed arm movements," *Experimental Brain Research*, vol. 172, no. 1, pp. 129–138, Jun 2006.

[18] D. R. Lametti, G. Houle, and D. J. Ostry, "Control of movement variability and the regulation of limb impedance," *Journal of Neurophysiology*, pp. 3516–3524, 2007.

[19] R. Osu, N. Kamimura, H. Iwasaki, E. Nakano, C. M. Harris, Y. Wada, and M. Kawato, "Optimal impedance control for task achievement in the presence of signal-dependent noise," *Journal of Neurophysiology*, vol. 92, no. 2, pp. 1199–1215, 2004.

[20] Y. Ueyama and E. Miyashita, "Signal-dependent noise induces muscle co-contraction to achieve required movement accuracy: A simulation study with an optimal control," *Current Bioinformatics*, vol. 8, pp. 16–24, 02 2013.

[21] P. L Gribble, L. I Mullin, N. Cothros, and A. Mattar, "Role of cocontraction in arm movement accuracy," *Journal of neurophysiology*, vol. 89, pp. 2396–405, 06 2003.

[22] J. Heald, D. Franklin, and D. Wolpert, "Increasing muscle co-contraction speeds up internal model acquisition during dynamic motor learning," *Scientific reports*, vol. 8, no. 1, 2018.

[23] K. A. Thoroughman and R. Shadmehr, "Electromyographic correlates of learning an internal model of reaching movements," *Journal of Neuroscience*, vol. 19, no. 19, pp. 8573–8588, 1999.

[24] N. Hogan, "Adaptive control of mechanical impedance by coactivation of antagonist muscles," *IEEE Transactions on automatic control*, vol. 29, no. 8, 1984.

[25] E. Burdet, D. W. Franklin, and T. E. Milner, "Chapter 4 - single-joint neuromechanics," in *Human Robotics - Neuromechanics and Motor Control*, 1st ed. Mit Press Ltd, 2013, pp. 57 – 78.

[26] D. Borzelli, B. Cesqui, D. J. Berger, E. Burdet, and A. D'Avella, "Muscle patterns underlying voluntary modulation of co-contraction." *Plos One*, vol. 13, pp. 1–30, 2018.

[27] R. Oldfield, “The assessment and analysis of handedness: The edinburgh inventory,” *Neuropsychologia*, vol. 9, pp. 97–113, 04 1971.

[28] D. Franklin, F. Leung, M. Kawato, and T. Milner, “Estimation of multijoint limb stiffness from emg during reaching movements,” *IEEE EMBS Asian-Pacific Conference on Biomedical Engineering*, pp. 224 – 225, 11 2003.

[29] P. Zaal, D. Pool, M. Mulder, and M. Paassen, “Multimodal pilot control behaviour in combined target-following disturbance-rejection tasks,” *Journal of Guidance, Control and Dynamics*, vol. 32, no. 5, pp. 1418–1428, 2009.

[30] K. Kording and D. Wolpert, “Bayesian integration in sensorimotor learning,” *Nature*, vol. 427, pp. 244–7, 02 2004.

[31] A. Takagi, M. Hirashima, D. Nozaki, and E. Burdet, “Individuals physically interacting in a group rapidly coordinate their movement by estimating the collective goal,” *eLife*, vol. 8, pp. 1–19, feb 2019.

[32] R. Osu, D. W. Franklin, H. Kato, H. Gomi, K. Domen, T. Yoshioka, and M. Kawato, “Short- and long-term changes in joint co-contraction associated with motor learning as revealed from surface emg,” *Journal of Neurophysiology*, vol. 88, no. 2, pp. 991 – 1004, 2002.

[33] B. Freriks and H. Hermens, *European recommendations for surface electromyography: results of the SENIAM project*. Roessingh Research and Development, 2000.

[34] P. L. Gribble, S. Everling, K. Ford, and A. Mattar, “Hand-eye coordination for rapid pointing movements,” *Experimental Brain Research*, vol. 145, no. 3, pp. 372–382, Aug 2002.

[35] N. W. Willigenburg, A. Daffertshofer, I. Kingma, and J. H. van Dieën, “Removing ecg contamination from emg recordings: A comparison of ica-based and other filtering procedures,” *Journal of Electromyography and Kinesiology*, vol. 22, no. 3, pp. 485 – 493, 2012.

[36] P. Konrad, *The ABC of EMG; A Practical Introduction to Kinesiological Electromyography*, 1st ed., April 2005.

[37] G. Frost, J. Dowling, K. Dyson, and O. Bar-Or, “Cocontraction in three age groups of children during treadmill locomotion,” *Journal of Electromyography and Kinesiology*, vol. 7, no. 3, pp. 179–186, 1997.

[38] J. Ropars, M. Lempereur, C. Vuillerot, V. Tiffreau, S. Peudenier, J. M. Cuisset, Y. Pereon, F. Leboeuf, L. Delporte, Y. Delpierre, R. Gross, and S. Brochard, “Muscle activation during gait in children with duchenne muscular dystrophy,” *PLoS ONE*, vol. 11, no. 9, pp. 1–13, 2016.

[39] S. C. Tseng, W. Liu, M. Finley, and K. McQuade, “Muscle activation profiles about the knee during Tai-Chi stepping movement compared to the normal gait step,” *Journal of Electromyography and Kinesiology*, vol. 17, no. 3, pp. 372–380, 2007.

[40] J. Z. Bakdash and L. R. Marusich, “Repeated measures correlation,” *Frontiers in psychology*, vol. 8, no. 456, 2017.

[41] A. Field, “Chapter 5 - exploring assumptions,” in *Discovering Statistics Using IBM SPSS Statistics*, 3rd ed. Sage Publications Ltd., 2009, pp. 162–164.

[42] R. Wilcox, “Chapter 10 - robust regression,” in *Introduction to Robust Estimation and Hypothesis Testing*, 3rd ed. Boston: Academic Press, 2012, pp. 471 – 532.

[43] P. L. Gribble and D. J. Ostry, “Independent coactivation of shoulder and elbow muscles,” *Experimental Brain Research*, vol. 123, no. 3, pp. 355–360, Nov 1998.

[44] D. W. Franklin, G. Liaw, T. E. Milner, R. Osu, E. Burdet, and M. Kawato, “Endpoint stiffness of the arm is directionally tuned to instability in the environment,” *Journal of Neuroscience*, vol. 27, no. 29, pp. 7705–7716, 2007.

[45] D. J. Reinkensmeyer, O. M. Akoner, D. P. Ferris, and K. E. Gordon, “Slacking by the human motor system: Computational models and implications for robotic orthoses,” in *2009 Annual International Conference of the IEEE Engineering in Medicine and Biology Society*, Sep. 2009, pp. 2129–2132.

[46] R. A. Scheidt, D. J. Reinkensmeyer, M. A. Conditt, W. Z. Rymer, and F. A. Mussa-Ivaldi, “Persistence of motor adaptation during constrained, multi-joint, arm movements,” *Journal of Neurophysiology*, vol. 84, no. 2, pp. 853–862, 2000.

[47] J. L. Emken, R. Benitez, A. Sideris, J. E. Bobrow, and D. J. Reinkensmeyer, “Motor adaptation as a greedy optimization of error and effort,” *Journal of Neurophysiology*, vol. 97, no. 6, pp. 3997–4006, 2007.

[48] A. Erdogan and V. Patoglu, “Slacking prevention during assistive contour following tasks with guaranteed coupled stability,” in *2012 IEEE/RSJ International Conference on Intelligent Robots and Systems*, Oct 2012, pp. 1587–1594.

[49] P. Artemiadis, “Chapter 11 - enhancing recovery of sensorimotor functions: The role of robot regenerated haptic feedback in the relearning process,” in *Neuro-Robotics: From Brain Machine Interfaces to Rehabilitation Robotics*. Springer, 01 2014, vol. 2, pp. 285–316.

[50] R. Osu, N. Kamimura, H. Iwasaki, E. Nakano, C. M. Harris, Y. Wada, and M. Kawato, “Optimal impedance control for task achievement in the presence of signal-dependent noise,” *Journal of Neurophysiology*, vol. 92, no. 2, pp. 1199–1215, 2004.

[51] B. Laursen, B. Jensen, and G. Sjogaard, “Effect of speed and precision demands on human shoulder electromyography during a repetitive task,” *European Journal of Applied Physiology*, vol. 78, no. 6, pp. 544–548, 1998.

[52] S. A. Baldauf, L. Engqvist, and F. J. Weissing, “Diversifying evolution of competitiveness,” *Nature Communications*, vol. 5, no. 1, 2014.

[53] A. Ma-Wyatt and S. P. McKee, “Initial visual information determines endpoint precision for rapid pointing,” *Vision Research*, vol. 46, no. 28, pp. 4675 – 4683, 2006.

[54] R. Shadmehr and S. Mussa-Ivaldi, “Chapter 10 - costs and rewards of motor commands,” in *Biological Learning and Control: How the Brain Builds Representations, Predicts Events, and Makes Decisions*. Mit Press Ltd, 2012, pp. 279 – 306.

[55] N. Hogan, “The mechanics of multi-joint posture and movement control,” *Biological Cybernetics*, vol. 52, no. 5, pp. 315–331, Sep 1985.

[56] C. DeLuca, “The use of surface electromyography in biomechanics,” *Journal of Applied Biomechanics*, vol. 13, pp. 135–163, 1997.

[57] T. E. Milner, “Dependence of elbow viscoelastic behavior on speed and loading in voluntary movements,” *Experimental Brain Research*, vol. 93, no. 1, pp. 177–180, 1993.

[58] E. Burdet, R. Osu, D. W. Franklin, T. Yoshioka, T. E. Milner, and M. Kawato, “A method for measuring endpoint stiffness during multi-joint arm movements,” *Journal of Biomechanics*, vol. 33, no. 12, pp. 1705–1709, 2000.

[59] D. J. Bennett, “Torques generated at the human elbow joint in response to constant position errors imposed during voluntary movements,” *Experimental Brain Research*, vol. 95, no. 3, pp. 488–498, 1993.

[60] D. Bennett, J. Hollerbach, Y. Xu, and I. Hunter, “Time-varying stiffness of human elbow joint during cyclic voluntary movement,” *Experimental Brain Research*, vol. 88, no. 2, pp. 433 – 442, 1992.

[61] F. Lacquaniti, M. Carrozzo, and N. Borghese, “Time-varying mechanical behavior of multijointed arm in man,” *Journal of Neurophysiology*, vol. 69, no. 5, pp. 1443 – 1464, 1993.

[62] D. Piovesan, P. Dizio, and J. R. Lackner, “A new time-frequency approach to estimate single joint upper limb impedance,” *Proceedings of the 31st Annual International Conference of the IEEE Engineering in Medicine and Biology Society: Engineering the Future of Biomedicine, EMBC 2009*, no. 3, pp. 1282–1285, 2009.

[63] D. Piovesan, A. Pierobon, P. Dizio, and J. R. Lackner, “Measuring multi-joint stiffness during single movements: Numerical validation of a novel time-frequency approach,” *PLoS ONE*, vol. 7, no. 3, 2012.

[64] D. Piovesan, P. Dizio, and J. R. Lackner, “Experimental measure of arm stiffness during single reaching movements with a time-frequency analysis,” *Journal of Neurophysiology*, vol. 110, no. 10, pp. 2484–2496, 2013.

[65] M. van de Ruit, J. Lataire, W. Mugge, G. Cavallo, J.-W. van Wingerden, A. C. Schouten, and F. C. T. van der Helm, “Revealing time-varying joint impedance with kernel-based regression and nonparametric decomposition,” *IEEE Transactions on Control Systems Technology*, pp. 1–14, 2018.

[66] R. Osu and H. Gomi, “Multijoint muscle regulation mechanisms examined by measured human arm stiffness and emg signals,” *Journal of Neurophysiology*, vol. 81, no. 4, pp. 1458–1468, 1999.

[67] H. Gomi and R. Osu, “Task-dependent viscoelasticity of human multijoint arm and its spatial characteristics for interaction with environments,” *Journal of Neuroscience*, vol. 18, no. 21, pp. 8965–8978, 1998.

[68] I. Hunter and R. Kearney, “Dynamics of human ankle stiffness: Variation with mean ankle torque,” *Journal of Biomechanics*, vol. 15, no. 10, pp. 747 – 752, 1982.

[69] H. Souissi, R. Zory, J. Bredin, and P. Gerus, “Comparison of methodologies to assess muscle co-contraction during gait,” *Journal of Biomechanics*, vol. 57, pp. 141–145, 2017.

[70] Y. Iwamoto, M. Takahashi, and K. Shinkoda, “Differences of muscle co-contraction of the ankle joint between young and elderly adults during dynamic postural control at different speeds,” *Journal of Physiological Anthropology*, vol. 36, no. 1, p. 32, 2017.

[71] D. A. Winter, *Biomechanics and Motor Control of Human Movement*, 4th ed. University of Waterloo, Waterloo, Ontario, Canada: John Wiley & Sons, Inc., 1990/2009, pp. 152-153.

[72] S. Balasubramanian, A. Melendez-Calderon, and E. Burdet, "A robust and sensitive metric for quantifying movement smoothness," *IEEE Transactions on Biomedical Engineering*, vol. 59, no. 8, pp. 2126–2136, Aug 2012.

[73] A. Sy and N. T. Bugtai, "Velocity and acceleration induced response to bicep emg signal threshold for motion intention detection," in *2014 International Conference on Humanoid, Nanotechnology, Information Technology, Communication and Control, Environment and Management (HNICEM)*, Nov 2014, pp. 1–6.

APPENDIX A
VISUAL NOISE PILOT STUDY

A. Introduction

To test if the amount of individual muscle co-contraction is related to the performance of one's partner, the tracking ability of participants should be manipulated to create a larger performance difference. This can be achieved by applying visual noise to the target [30], [31]. To understand the effect of visual noise on the individual motor performance, a pilot study was executed.

B. Method

Three participants (aged 23-32, 1 female, 2 males; two where right-handed according to the Edinburgh handedness inventory [27]) participated in the experiment. All participants where naïve to the visual noise task. The experiments were performed using one manipulandum of the robotic setup mentioned in section II-A (see Fig. 1). All participants performed the same planar tracking task. The goal was to track the target as accurately as possible. The participants tracked the continuously moving target during trials of 20 s followed by a 5 s break. The monitor displayed a cursor of the handle position and the target, which was composed of a dynamical cloud. The target movement (in cm) was defined as a sum-of-sines [6]:

$$\begin{aligned} x(t) &= 2.87\sin(0.94t - 7.77) + 2.71\sin(1.26t - 8.53), \\ &\quad + 2.35\sin(1.89t - 4.36) + 1.80\sin(2.83t - 3.79), \\ y(t) &= 2.71\sin(1.26t - 0.71) + 2.53\sin(1.57t - 3.79), \\ &\quad + 2.16\sin(2.20t + 2.92) + 1.64\sin(3.14t + 4.93). \end{aligned} \tag{A.1}$$

The tracking signal required hand movements over a circular workspace with a radius of 10 cm, an average of 7.9 cm s^{-1} and a maximum velocity of 13.9 cm s^{-1}. To prevent fast learning or other cognitive strategies, an uniformly random start time for the signals was chosen ($t \in [t_0, t_0 + 20]s$). The dynamic cloud consisted of five circular spots that were displayed every millisecond. Each spot was regenerated, one at a time, every 500 ms by picking a new relative position and velocity with respect to the target. The absolute spot velocity was defined as the sum of the target velocity and the assigned relative spot velocity:

$$\begin{aligned} \dot{x}_{s_i}(t) &= \dot{x}(t) + \Delta\dot{x}_{s_i}, \\ \dot{y}_{s_i}(t) &= \dot{y}(t) + \Delta\dot{y}_{s_i}, \end{aligned} \tag{A.2}$$

where $\Delta\dot{x}_s$ and $\Delta\dot{y}_s$ are the assigned relative spot velocities (regenerated every 500 ms) and subscript i denotes the considered spot ($i \in [1, 5]$). The position and velocity parameters were determined from normal random distributions with a standard deviation of 0.4 cm for the position, and from a set of thirteen values for the velocity (ten equally spaced values from 0.5 to 30 cm s^{-1} and 15, 22.5 and 30 cm s^{-1}). Spots with low velocity noise where easy to track but high velocity noise spots spread out rapidly like fireworks. Each participant performed four blocks of fifteen trials. Between blocks participants had a two-minute break. The first eight trials served as a baseline, in which the target was visualized as one spot with no visual noise. In the following 52 trials, the standard deviation of the velocity varied per trial. Each level of noise was tested for four trials, randomly ordered. The tracking error of each participant in a trial was measured as the root-mean squared distance between the target and the cursor. The lower the tracking error, the better the performance.

C. Results

Fig. 11 shows the tracking error of all three participants as a function of the different levels of visual noise. There is a significant relationship between the standard deviation of the relative spots' velocities and the tracking error, $r = \begin{bmatrix} .95 & .91 & .92 \end{bmatrix}$, p (one-tailed) < 0.001. The tracking error increased linearly with respect to an increasing standard deviation of the relative spots' velocities up to a certain level of visual noise. Above a standard deviation of approximately 10 cm s^{-1} the effect of an increasing standard deviation of the relative velocity starts to decline.

D. Conclusion

The tracking error of participants is linearly and tightly related to the standard deviation of the visual noise up to a standard deviation of approximately 10 cm s^{-1}. Visual noise can therefore be used to influence the tracking performance of the participants.

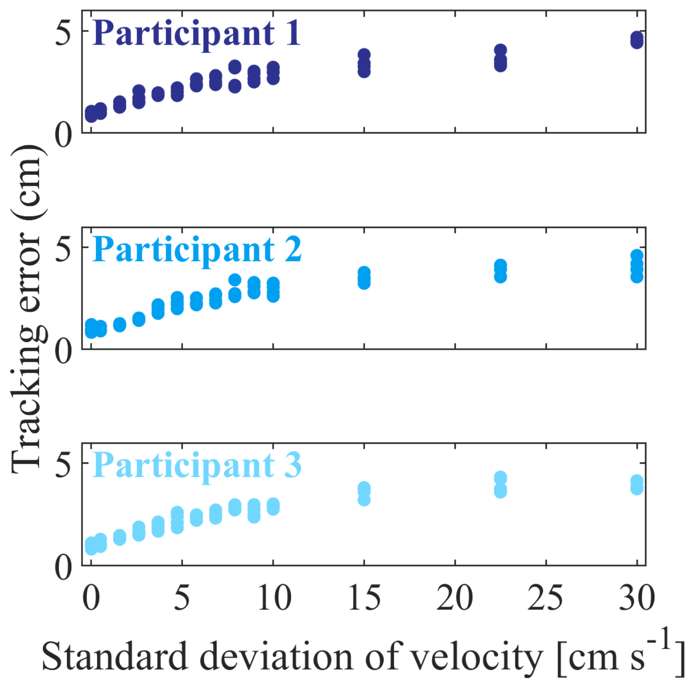

Fig. 11. Standard deviation of the relative spots' velocities versus the tracking error. Each level of noise was tested for four trials.

APPENDIX B
DESIGN OF PROTOCOL

A. Number of trials

At the start of each connected trial a certain standard deviation for the velocity of the spots within the dynamic cloud is assigned to the participants. One of the two participants is always assigned with the smallest standard deviation for the velocity while the other participant is assigned with one of the included standard deviations for the velocity. The number of possible combinations for a connected trial (connected conditions) is therefore two times the amount of standard deviations for the velocity minus one. EMG signals are variable as they are a result of many physiological, anatomical and technical factors [56]. Because of this, each connected condition is repeated five times. The amount of single trials is equivalent to the amount of standard deviations for the velocity. The single conditions are repeated five times. The total amount of trials (n_{trials}) depends on the amount of included standard deviations for the velocity:

$$n_{trials} = n_{training} + 5(2n_{sd} - 1) + 5n_{sd}, \tag{B.1}$$

where $n_{training}$ is the amount of training trials and n_{sd} the amount of included standard deviations for the velocity. To limit the experimental time, a maximum of 90 trials, including 20 training trials, is chosen. To satisfy this criterion, the amount of included standard deviations for the velocity is set to five.

B. Trajectory

The target signal is designed as quasi-random sum-of-sine signals with sines at multiple frequencies [29]. The random appearance of such multi-sine signals induces skill-based feedback control behaviour, while allowing the experiment designer to define the properties of the signal [29]. The target signal is designed according to:

$$\begin{aligned} x(t) &= \sum_{k=1}^{N} A_x(k)\sin(\omega_x(k)t + \varphi_x(k)), \\ y(t) &= \sum_{k=1}^{N} A_y(k)\sin(\omega_y(k)t + \varphi_y(k)), \end{aligned} \tag{B.2}$$

where $A(k)$, $\omega(k)$ and $\varphi(k)$ indicate the amplitude, frequency and phase of the k^{th} sine. N indicates the number of sines which is set to four. In every trial a measurement time of $T_m = 20$ s is used. The sinusoid frequencies $\omega_x(k)$ and $\omega_y(k)$ are all defined to be integer multiples of the measurement time base frequency, $\omega_m = 2\pi/T_m = 0.3142$ rad/s. The multiples are chosen in such a way that the mean velocity of the target is ± 12 cm s^{-1}. The amplitudes of the individual sines are determined with a second-order low-pass filter:

$$A(j\omega) = \left| \left(\frac{1 + T_{A1}j\omega}{1 + T_{A2}j\omega}\right)^2 \right|, \tag{B.3}$$

with $T_{A1} = 0.05$ s and $T_{A2} = 0.42$ s. Such a filter reduces the power for the higher frequencies, giving a realistic and not overly difficult tracking task. The amplitude distributions of A_x and A_y were scaled to attain different variances for x and y (ratio of 4:3) to create larger differences between the amplitudes. Besides, the amplitudes where scaled to a maximum deviation of 9.5 cm. A large number of random sets of phases was generated to determine the phase distribution. The two sets of phases that yielded the smoothest path, without leading to excessive peaks, were selected for x and y. This set was chosen to minimize the crest factor for x and y:

$$\begin{aligned} CF_x &= \frac{max|x(t)|}{\sigma_x}, \\ CF_y &= \frac{max|y(t)|}{\sigma_y}, \end{aligned} \tag{B.4}$$

where σ_x and σ_y are the standard deviations of the signal x and y, respectively. Besides the curvature was minimized:

$$\kappa = \frac{|\ddot{x}\dot{y} - \dot{x}\ddot{y}|}{(\dot{x}^2 + \dot{y}^2)^{3/2}}. \tag{B.5}$$

APPENDIX C
MEASURING CO-CONTRACTION

This section discusses possible methods to measure muscle co-contraction and the applicability in a continuously tracking task during haptic human-human interaction. Thereafter the chosen method is discussed.

A. Mechanical perturbations

Co-contraction of antagonistic muscles causes an increase in both the stiffness and viscosity of the joints. Several studies measured joint stiffness using mechanical force perturbations [57] or position perturbations [58], [59]. These methods use force/torque or position perturbations and measure the resulting change in displacement or restoring force relative to the mean undisturbed movement for force/torque and position perturbations, respectively. The relative displacement or restoring force are then used to determine joint stiffness. These methods require knowledge of the unperturbed trajectory which implies that the trajectory should be repeatable and not change over trials. Because of the interaction forces during haptic interaction, this assumption cannot be made.

B. System identification

Bennett [60] and Lacquanti [61] used system identification with a linear second-order model to measure joint stiffness with force perturbations as input and the displacement as output. These methods require continuous mechanical perturbations as an input which will disturb the interaction forces. Besides, multiple repeated trials are needed for a reliable estimation which will make the experiment very long.

C. Time-frequency approach

Piovesan et al. [62]–[64] used time-frequency analysis to estimate the arm's mechanical properties along a reaching trajectory. The method is based on the analysis of the reassigned spectrogram of the arm's response to impulsive perturbations and can estimate arm stiffness on a trial-by-trial basis. Van der Ruit et al. [65] used a different time-frequency approach. They validated a parametric and non parametric estimator to identify continuous-time linear time-varying systems. The parametric estimator is based on a kernel based regression method and the non parametric estimator is based on a skirt decomposition method. The advantage of nonparametric models over parametric models is that they require very little to no apriori assumptions on the model structure and order. These methods, however, require continuous mechanical perturbations as an input which will disturb the interaction forces.

D. Electromyography

Osu et al. [32], [50] proposed an index of muscle co-contraction around the joint (IMCJ) computed from surface EMG and joint torques. They based their method on the evidence that static stiffness and surface EMG [66] and joint stiffness and joint torque [67], [68] are highly correlated. This method assumes linear length-tension and velocity-tension curves and constant moment arms. These simplifications lead to an error which are only negligible if the movement of an individual is identical in all trials which is not the case in a haptic interaction experiment due to the interaction forces.

Gribble et al. [21] measured the level of co-contraction by normalising each muscle's EMG activity by its maximum value. They discarded the portion of EMG in one muscle that is not matched by EMG in the opposing antagonistic muscle. The resulting time-varying signal represented the magnitude of EMG that is equal and opposite in antagonistic muscles [23]. Besides, several studies investigated the changes in muscle activity during gait and quantified the level of co-contraction with a co-contraction index [69]. The level of co-contraction is monitored by the normalised EMG activity of the antagonistic muscles and is the common area of activity either absolute [37]–[39] or relative [70], [71]. The relative co-contraction index is most suitable when using the index to determine the efficiency of a movement. The absolute co-contraction index is most suitable when looking for differences in the amount of co-contraction.

E. Chosen method

The used method in the experiment is based on the method of Gribble et al. [21] using the absolute co-contraction index described in gait analysis studies [37]–[39]. The absolute co-contraction index is calculated as

$$CI = \frac{1}{n}\sum_{i=1}^{n}(\text{common area muscle } A \text{ \& } B), \tag{C.1}$$

where muscle A and B represent the antagonistic muscles. To enlarge the effect of peaks in the common area and thus the level of co-contraction, the root mean square is used instead of the mean

$$CI = \sqrt{\frac{1}{n}\sum_{i=1}^{n}(\text{common area muscle } A \text{ \& } B)^2}. \tag{C.2}$$

APPENDIX D
EFFECT OF VISUAL NOISE ON THE INDIVIDUAL MOTOR PERFORMANCE

This section discusses the influence of visual noise on the individual performance. The first subsection discusses the influence of the level of visual noise in the previous trial on the performance in the successive trial. Thereafter, the effect of visual noise on the smoothness of the movement of participants is examined. Finally, the effect of visual noise on the mean velocity and acceleration is analysed.

A. *Visual noise level in previous trial*

Visual noise impairs the belief about the position of the target and therefore introduces lower accuracy in the performance. Because the level of visual noise changed randomly within the experiment, it is possible that the level of visual noise of the previous trial had an effect on the performance of the participants in the successive trial. To investigate this, the deviation from the mean error per level of visual noise experienced in the previous trial is calculated as

$$\Delta E_{i,k,j} = \frac{\overline{E_{i,k,j}}}{\overline{E_{k,j}}}, \tag{D.1}$$

where $\overline{E}$ denotes the mean error and i, k and j the level of visual noise of the previous trial, the level of visual noise of the successive trial and the participant, respectively. Fig. 12 shows the deviation from the mean error as a function of the level of visual noise in the previous trial. An ANOVA test showed that there is no significant difference in the deviation from the mean error with respect to the level of visual noise in the previous trial ($F(4, 333) = 0.43$, $p > 0.79$). The level of visual noise in the previous trial has thus no influence on the performance in the successive trial.

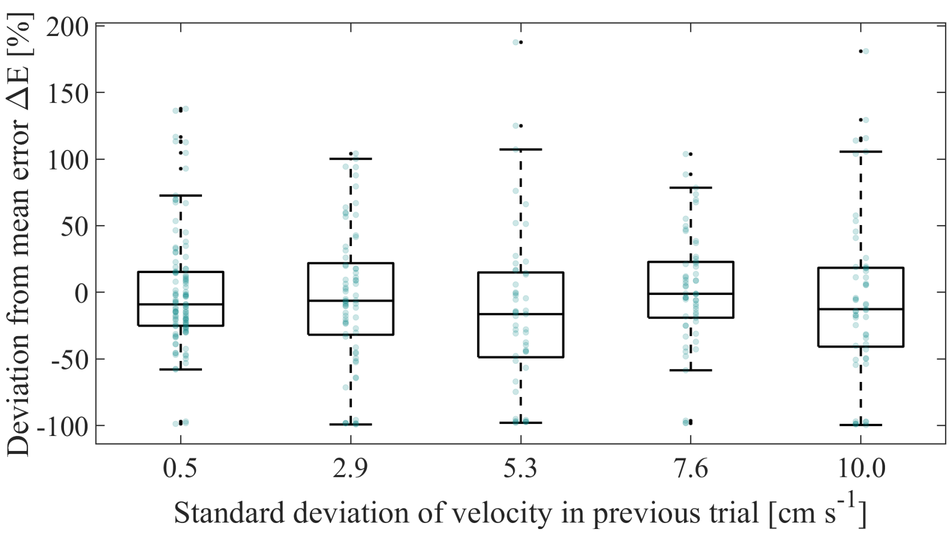

Fig. 12. The deviation from the mean error is plotted as a function of the level of visual noise in the previous trial. The green data points represent an individual participant.

B. *Smoothness*

A higher level of visual noise might cause less smoother movements within a trial because predictions about the position of the target are less accurate. The smoothness of the movement of each participant is calculated as the spectral arc length of the velocity [72]. Fig. 13 shows the smoothness as a function of the level of visual noise. A repeated measures ANOVA test showed that the smoothness does not significantly changed with respect to the level of visual noise ($F(4, 84) = 1.34$, $p = 0.26$).

C. *Velocity and acceleration*

To check if the increased amount of common area in EMG activity due to the lowest level of visual noise ($\sigma_v = 0.5\ \mathrm{cm\,s^{-1}}$) is not caused by a change in mean velocity or acceleration, a paired-samples t-test and in case of non-normality a non-parametric Wilcoxon signed rank test is performed. It appeared that the mean velocity in the lowest level of visual noise is decreased with respect to all other levels of visual noise ($t = -2.65$, $p = 0.015$). No significant difference in the mean acceleration between the levels of visual noise is found ($z = -0.828$, $p = 0.41$). The study of Sy and Bugtai [73] showed that a larger

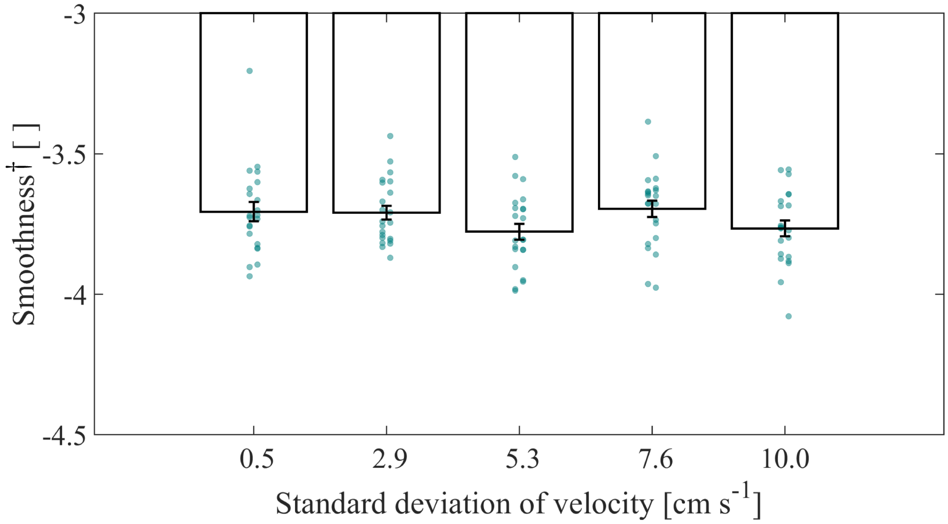

Fig. 13. The smoothness is plotted as a function of the level of visual noise. The green data points represent an individual participant. † To account for individual differences, the smoothness (S) is adjusted: $S_{adjusted_{i,p}} = S_{i,p} + (\frac{1}{P}\sum_{p=1}^{P}\overline{S}_g - \frac{1}{N}\sum_{i=1}^{N} S_{i,p})$, where n and p denote the trial number and participant number, respectively, and $\overline{S}_g$ denotes the mean smoothness of each participant.

velocity resulted in a higher amount of EMG activity. Because the velocity decreased when the amount of common area in EMG activity increased for the lowest level of visual noise, this effect is caused by an increase in co-contraction.

Appendix E
Co-contraction index as a function of partner performance

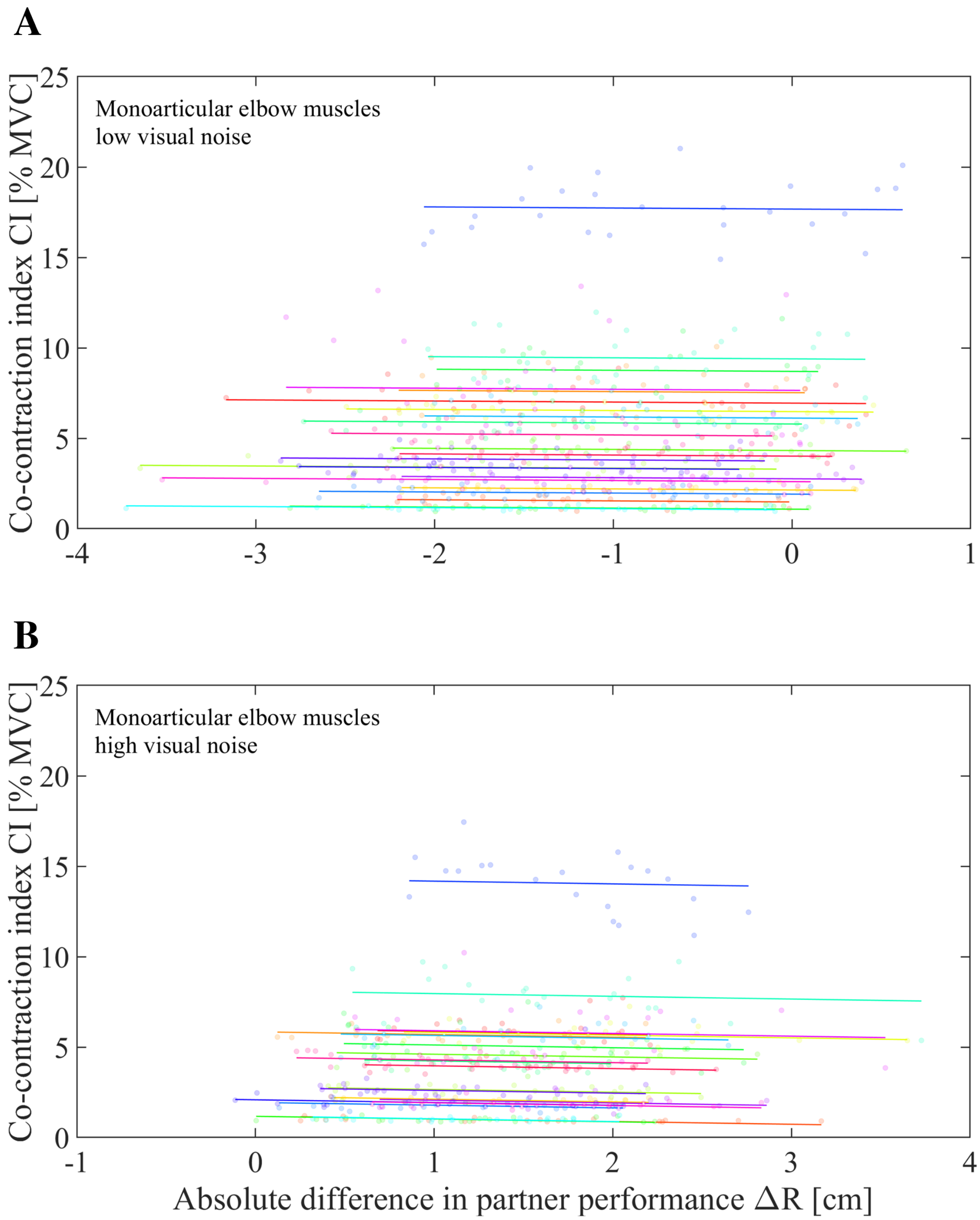

Fig. 14. The co-contraction index of the monoarticular elbow muscles during interaction as a function of the absolute difference in partner performance. Each color represents a specific participant. Data points are fitted using a linear mixed model with a random intercept and fixed slope. **A** Data points are measured when a low level of visual noise was applied to the target ($\sigma_v = 0.5$ cm s^{-1}). **B** Data points are measured when a high level of visual noise was applied to the target ($\sigma_v = 2.9, 5.3, 7.6, 10$ cm s^{-1}).

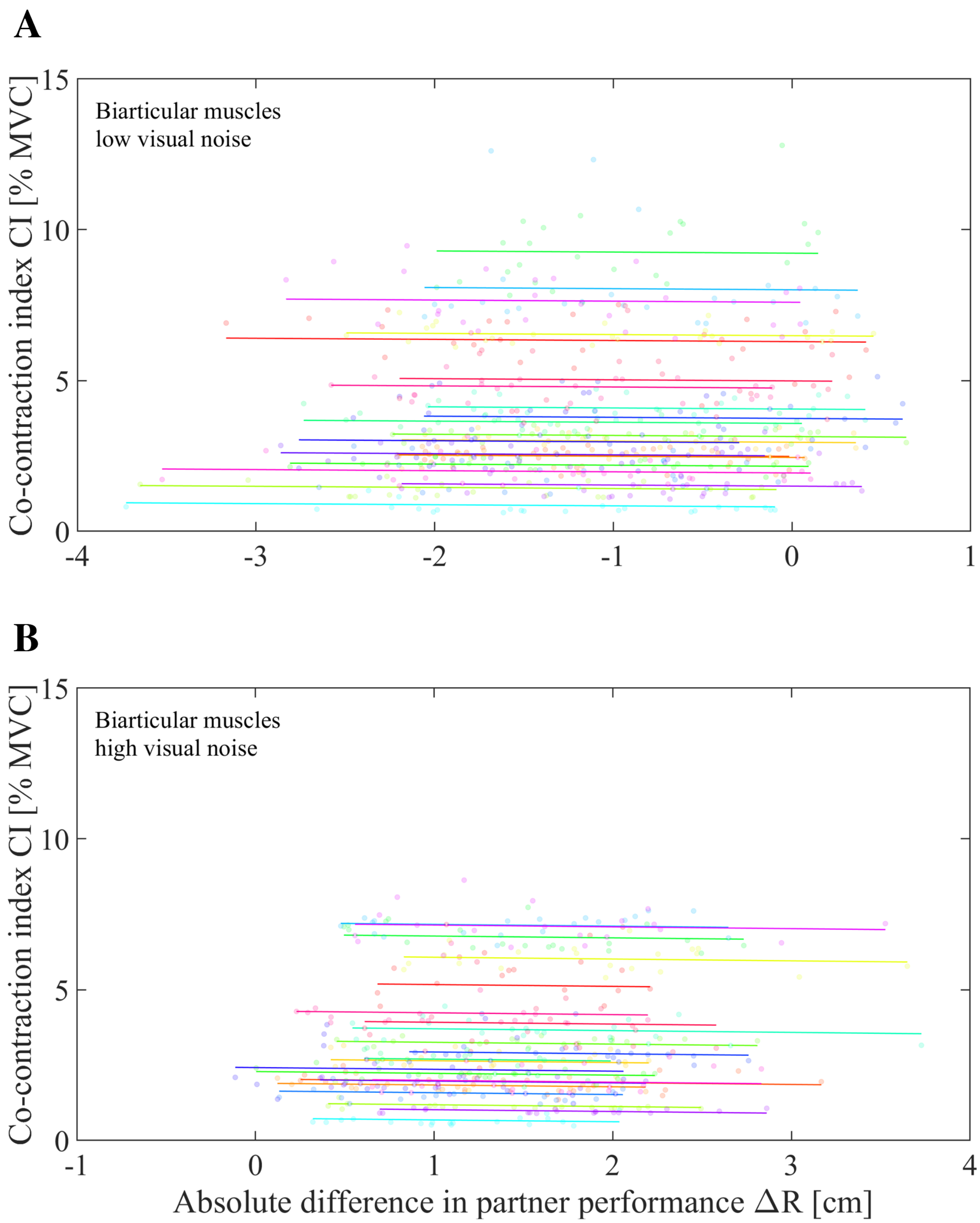

Fig. 15. The co-contraction index of the biarticular muscles during interaction as a function of the absolute difference in partner performance. Each color represents a specific participant. Data points are fitted using a linear mixed model with a random intercept and fixed slope. **A** Data points are measured when a low level of visual noise was applied to the target ($\sigma_v = 0.5$ cm s^{-1}). **B** Data points are measured when a high level of visual noise was applied to the target ($\sigma_v = 2.9, 5.3, 7.6, 10$ cm s^{-1}).